UNIVERZITA PALACKÉHO V OLOMOUCI

PŘÍRODOVĚDECKÁ FAKULTA

KATEDRA BIOFYZIKY

DIPLOMOVÁ PRÁCE

Umělé hlasivky pro experimentální výzkum tvorby hlasu

Autor: Bc. Michal Berecka

Studijní obor: Biofyzika

Vedoucí bakalářské práce: doc. RNDr. Jan Švec, Ph.D. et Ph.D.

Olomouc 2023

PALACKÝ UNIVERSITY OLOMOUC

FACULTY OF SCIENCE

DEPARTMENT OF BIOPHYSICS

DIPLOMA THESIS

Artificial Vocal Folds for Experimental Research of Voice Production

Author: Bc. Michal Berecka

Study programme: Biophysics

Supervisor: doc. RNDr. Jan Švec, Ph.D. et Ph.D

Olomouc 2023

Souhrn

Jméno a příjmení autora: Bc. Michal Berecka

Název práce: Umělé hlasivky pro experimentální výzkum tvorby hlasu

Typ práce: Experimentální

Pracoviště: Laboratoř výzkumu hlasu, Katedra experimentální fyziky

Vedoucí práce: doc. RNDr. Jan Švec, Ph.D. et Ph.D.

Konzultant: Ing. Petr Hájek, Ph.D.

Rok obhajoby práce: 2023

Abstrakt:

Diplomová práce je zaměřena na vývoj umělých hlasivek a jejich podpůrné struktury pro použití ve studiu tvorby hlasu. Podpůrná struktura hlasivek byla navrhnuta tak, aby ji bylo možné použít s částmi experimentálního zařízení pro studium tvorby hlasu, které již byly dříve vyrobeny pro studium fonací preparátu hrtanu. Dalším cílem bylo, aby byla podpůrná struktura hlasivek modulární, tedy aby její části mohli být jednoduše a levně vyměněny za jiné části. Byl vytvořen návod na výrobu modelů hlasivek a také nástroje, které tuto výrobu usnadňují. Několik těchto modelů bylo testováno pro jejich schopnost samobuzené oscilace. Finální verze modelů silikonových hlasivek vykázala schopnost samobuzených oscilací na frekvencích 59-90 Hz, které jsou na dolní hranici frekvencí kmitů pozorovaných u mužských hlasivek *in vivo*.

Klíčová slova: umělý hrtan, model hlasivek, samobuzený model hlasivek, fonace

Počet stran: 57

Jazyk: Anglický

Summary

Author´s first name and surname: Bc. Michal Berecka

Title of thesis: Artificial vocal folds for experimental research of voice production

Type of thesis: Experimental

Department: Voice Research Laboratory, Department of Experimental Physics

Supervisor: doc. RNDr. Jan Švec, Ph.D. et Ph.D.

Consultant: Ing. Petr Hájek, Ph.D.

The year of defence: 2023

Abstract:

The diploma thesis focuses on development of silicone models of vocal folds and their supporting framework to be used in studying of voice production. The supporting framework was designed to be used with parts of an experimental setup that were previously developed and manufactured for studies of phonation in excised larynges. The supporting framework was made to be modular, with parts being replaceable easily and without high financial costs. A step-by-step manual of vocal fold model fabrication was created, along with several devices used to help during the fabrication. Selected models were tested for their ability of self-oscillation. The final versions of the silicone vocal folds exhibited the ability to self-oscillate at the frequencies of 59-90 Hz. These frequencies are at the lower boundary of the oscillatory frequencies observed in male human vocal folds *in vivo*.

Key words: artificial larynx, vocal fold model, self-oscillating vocal fold model, phonation

Number of pages: 57

Language: English

Rád bych poděkoval doc. RNDr. Janu Švecovi, Ph.D. et Ph.D. za jeho dozor, vedení a rady jak při psaní diplomové práce, tak při experimentální práci v laboratoři. Také bych rád poděkoval Ing. Petru Hájkovi, Ph.D. za pomoc, rady a spolupráci při modelování i experimentální práci. Další poděkování patří Mgr. Lukáši Kouřilovi, Ph.D. za 3D tisk, Ing. Anně Hrubanové za měření materiálů a Hugo Lehouxovi, M.Sc. za pomoc v laboratoři.

I would like to thank doc. RNDr. Jan Švec, Ph.D. et Ph.D., for his supervision, guidance and advice both during the writing of the thesis and in laboratory. I would also like to thank Ing. Petr Hájek, Ph.D. for his help, advice and cooperation with modelling and experimental work. Additional thanks belong to Mgr. Lukáš Kouřil, Ph.D. for 3D printing, Ing. Anna Hrubanová for material tests and Hugo Lehoux M.Sc. for his help in the laboratory.

CONTENT

1. INTRODUCTION

This thesis focuses on vocal fold models and their usage in studies of phonation and on supporting frameworks and the experimental setups used to study voice production in general.

The sound known as human voice is a result of a physical process known as phonation. The human voice is produced by oscillation of the vocal folds, which are part of a system responsible for phonation that can be divided into three parts – the lungs, the vocal folds, and the vocal tract. The lungs provide air pressure and air flow, which is modulated by the oscillation of the vocal folds and refined by the vocal tract.

The vocal folds are located inside larynx, which can be divided into two parts, hard tissue consisting of cartilages and soft tissue, consisting of muscles and ligaments. The vocal folds have an integral structure that is usually divided into three layers with different elastic properties – epithelium, lamina propria and vocalis muscle.

Vocal fold models can be divided into two main groups, mathematical models, which rely on mathematical equations and their calculations, and physical models, using either artificial or dissected vocal folds. The artificial vocal fold models can be divided into three categories – static models, externally driven models, and self-oscillating models. Static models were the first and simplest models developed, they use rigid vocal folds, that do not vibrate or move and function more akin to barrier for the airflow. The externally driven models feature moving vocal folds, however; the vocal folds oscillation is externally controlled, as opposed to real vocal folds, which self-oscillate. The self-oscillating models use synthetic materials with properties similar to real human vocal folds, which are capable of self-oscillation and voice production without externally moving them.

This thesis is divided into three main parts. The theoretical part focuses on vocal folds, their properties and divisions, vocal fold models and their categories and vocal fold model fabrication in literature. Methodical part focuses on materials and methods used in the experimental setup´s and vocal fold model´s development and fabrication. The results and discussion part focuses on the development and final version of the supporting framework, the fabrication of the vocal fold models and the testing of the vocal fold models ability of self-oscillation and thus phonation.

2. THEORY

2.1 Voice production

The sound known as human voice is the result of a physical process known as phonation (Kniesburges *et al*. 2011). The human voice is produced by oscillation of the vocal folds, which are part of a system responsible for phonation (Figure 1), that can be divided into three parts – the lungs, the vocal folds and the vocal tract (Zhang 2016).

The function of the lungs and the lower airways is to provide air pressure and airflow. The airflow is then modulated by the oscillation of the vocal folds and refined by the vocal tract, a set of cavities, that function as an acoustic filter modifying the spectrum of the sound (Pulakka 2005). The lungs and the lower airways thus in this three-part system act as a source of airflow, the vocal folds act as a primary generator of sound using the airflow to produce the sound and the vocal tract acts as a filter shaping the primary sound into the final sound (Andrade 2015).

The air expired from the lungs provides energy necessary for vibration of the vocal folds, however, the energy dissipates during vibration due to tissue viscosity, therefore the energy needs to be added for vocal fold oscillations to be self-sustainable. According to the myoelastic-aerodynamic theory of phonation, the vibratory characteristics are dependent mainly on elastic properties of vocal folds, which can be changed by laryngeal muscles (Švec *et al.* 2021). When several conditions are met, such as certain subglottal pressure and tensions in vocal muscles, the vocal folds begin oscillating producing sound (Šidlof 2007).

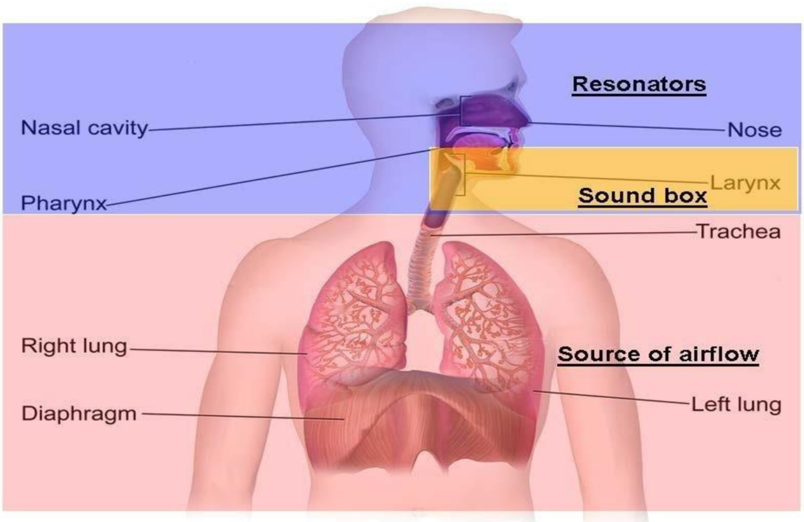

Figure 1: Voice production system. Taken from Andrade (2015) originally from Blausen.com.

2.2 Vocal folds

The vocal folds are located inside larynx, which can be divided into two parts, hard tissue and soft tissue. Hard tissue consists of cartilages and forms a structure to which the soft tissue is connected. These cartilages are thyroid cartilage, cricoid cartilage, epiglottis, a pair of corniculate cartilages and a pair of arytenoid cartilages (Figure 2). The vocal folds are attached to the arytenoid cartilages at the back and at their front, they are attached to thyroid cartilage.

Soft tissue is primarily made of muscles, such as cricothyroid muscle and thyroarytenoid muscles, and ligaments. The activity of larynx muscles plays a major role for phonation, the muscles are responsible for multitude of function, such as the movement of cartilages, which causes abduction and adduction of the vocal folds and adjust the inner tension of the vocal folds.

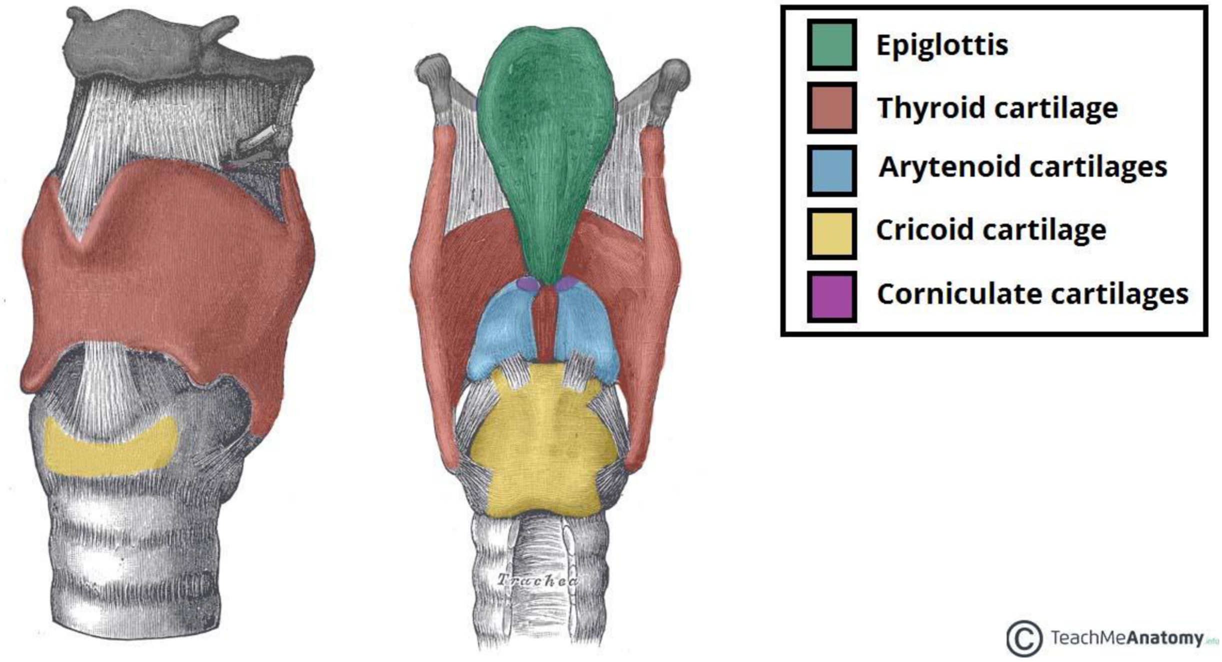

Figure 2: Laryngeal cartilages. Taken from www.teachmeanatomy.info.

2.2.1 Structure of the vocal folds

The structure of the vocal folds can be divided into three parts, epithelium, lamina propria and vocalis muscle (Figure 3) (Miri 2014).

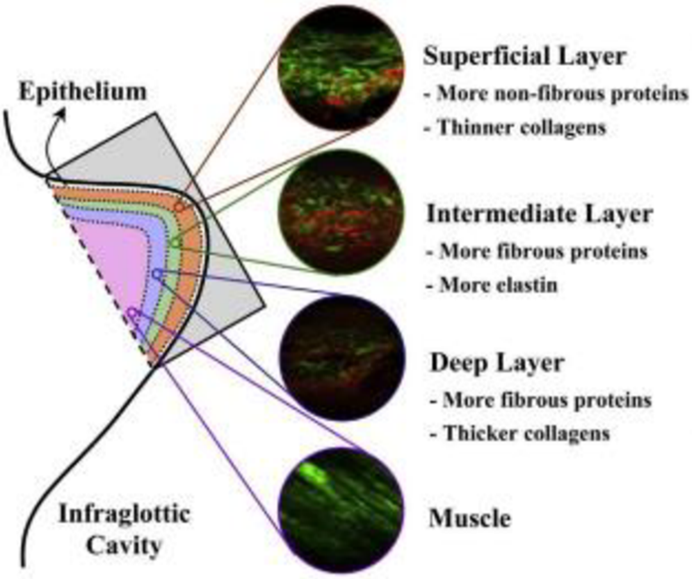

Figure 3: The structure of the vocal folds. Taken from Miri (2014), cropped.

The epithelium covers the surface of the vocal folds and is made of five to ten layers of closely packed stratified squamous cells (Arens *et al.* 2007). The individual layers of the epithelium can be further grouped into basal layer and suprabasal layer (Figure 4), where the basal layer is directly adjacent to the basement membrane (Levendoski *et al.* 2014). The basement membrane contains collagenous anchoring structures, which help secure the epithelium to the lamina propria (Gray *et al.* 1997).

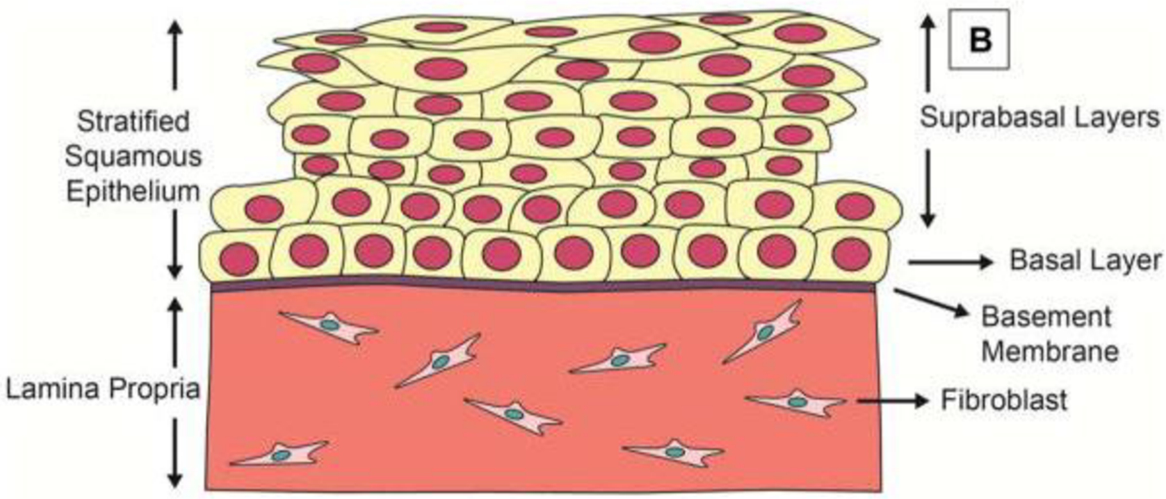

Figure 4: Structure of the vocal fold epithelium. Taken from Levendoski et al. (2014), cropped.

The lamina propria is usually divided into three layers: superficial layer, intermediate layer and deep layer (Hirano 1981). The superficial layer, also called Reinke's space, is the outermost layer of the lamina propria, it is roughly 0,5 mm thick and is made of unorganized elastin fibres. The intermediate layer is also primarily composed of elastin fibres, but the fibres are organized - in anterior-posterior direction. The primary component of the deep layer are collagen fibres that, in contrast to elastin fibres are very rigid (Colton 1988).

Lamina propria's deep layer is connected to the thyroarytenoid muscle, which forms the rigid body of the vocal folds. The thyroarytenoid muscles activity is responsible for the changes in inner tension of the vocal folds, which plays an important in phonation, its other main function is to keep the vocal folds together against the airstream.

2.2.2 Systems of structure division in vocal folds

The structure of the vocal folds can be divided based on the intended application. The basic division of the vocal folds is into three parts – epithelium, lamina propria and thyroarytenoid muscle. Additionally, the lamina propria is usually divided into its own three parts (Hirano 1981) forming the five-part division system consisting of epithelium, superficial layer of lamina propria, intermediate layer of lamina propria, deep layer of lamina propria and thyroarytenoid muscle.

Hirano (1974) proposed the cover-body division of the vocal folds, the system was later extensively used in kinetic analysis of vocal fold vibrations. In this division system, the epithelium, the superficial layer and the intermediate layer of lamina propria are grouped into one part called the cover and the deep layer and the thyroarytenoid muscle are grouped together into part called body.

Last division system divides the vocal folds into three layers of similar elastic properties and is often used in both physical and mathematical models. The first layer is usually called mucosa and groups together the epithelium with the superficial layer of lamina propria, the second layer is called ligament and consists of the intermediate and the deep layer of lamina propria. The third and last layer is the thyroarytenoid muscle.

2.2.3 Elastic properties of the vocal folds

Layers of the vocal folds have different elastic properties based on their composition; these properties are usually characterized by Young's modulus. The Youngs modulus in vocal folds decreases with the depth, thus the deeper parts of the vocal folds, such as the muscle have lower Young's modulus than the surface parts, such as the epithelium (Figure 5).

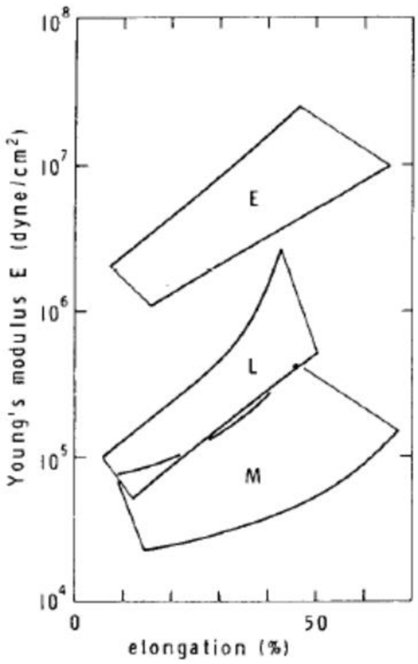

Figure 5: Young's modulus related to elongation of epithelium (E), ligament (L) and muscle (M) in the three-part division system of the vocal fold. Taken from Kakita et al. (1981).

The Young's modulus for the entire vocal fold without division is difficult to obtain as it is dependent on many factors; for example, the difference between no strain and 25% strain on the vocal folds significantly changes the Young's modulus (Thomson 2004).

The overall Young's modulus of the vocal folds can either be taken as an average of measured Young's moduli of individual parts or the entire vocal fold Young's modulus can be measured as one piece. The mean value of the transverse Young's modulus of human vocal folds was measured to be 12.7 kPa (Tran *et al.* 1993). In the article published by Becker *et al.* (2009) the authors provided a table with basic physical parameters of the vocal folds used for investigation of the human voice with Young's modulus values being between 5 and 10 kPa.

2.3 Vocal fold models

Studying phonation *in vivo* comes with many limitations causing the need for vocal fold models. The usage of human vocal folds is theoretically possible; however, it comes with technical and ethical obstacles. To overcome these obstacles, two groups of vocal fold models were devised, the physical models, where the human vocal folds are substituted for synthetic variants and mathematical models.

2.3.1 Mathematical vocal fold models

The mathematical models rely on mathematical equations and their calculations. As these calculations are very complex, it became clear early on, that their solving requires the use of computers. The basic model for mechanical description in voice production is a two-mass nonlinear oscillator system (Ishizaka and Flanagan 1972), this model can further be upgraded into three or more mass systems, or even simplified into a one-mass system (Cveticanin 2012). The mathematical models corresponding to the above-mentioned mechanical models are systems of coupled second-order differential equations, which describe the vibrations of the vocal folds.

Mathematical models studying the vibrations of the vocal folds are very good at providing qualitative results. However even though clinically observed and measured parameters are used for modelling, quantitative results of these models differ from the real results (Cveticanin 2012). De Boer and Fitch (2010) stated that the mathematical models are best used along with experimental studies as they complement each other.

One of their biggest advantages is the option to focus on specific aspects of phonation, which is harder to achieve using physical models. The option to study the vocal fold vibrations in variable simulated conditions as opposed to the physical models can be very useful in studies, where the realistic conditions are hindering the results and are not overly important. However, in many studies, the inclusion of realistic conditions is important, which is much harder to achieve using mathematical models.

2.3.2 Physical vocal fold models

The physical models of vocal folds use either artificial or dissected vocal folds and larynges to study the phonation. Over the years, many different types of artificial models were developed and used, these models can be classified into three main groups – a) static models with fixed rigid vocal folds, b) externally driven models, using externally driven vocal folds and c) self-oscillating synthetic fully-coupled models. (Kniesburges *et al.* 2011).

2.3.2.1 Static models

Static vocal fold models were the first and the simplest models to be used and developed by researchers for replication of the vocal fold shape using variety of materials, such as brass (Wegel 1929) or later by using canine larynx plaster casts (van der Berg *et al.* 1957) An overview of these can be found in Kniesburges *et al.* (2011).

Static models use rigid vocal folds, usually with upscaled geometry. The vocal folds in these models do not vibrate or move and their function is more akin to a barrier for airflow rather than phonation. Therefore, static models have not been used for experiments studying vibrations and voice production but have been rather focused on aerodynamic studies of parameters such as intraglottal pressure or air flow.

In the early 2000s Scherer *et al.* (2000) developed and used a static model called M5. This model, primarily its vocal fold geometry, has since been extensively used and built upon. The original M5 model was a Plexiglas model of a simplified larynx (Figure 6); the linear dimensions were 7.5 times greater than the physiological dimensions of male larynx (Scherer *et al.* 2001).

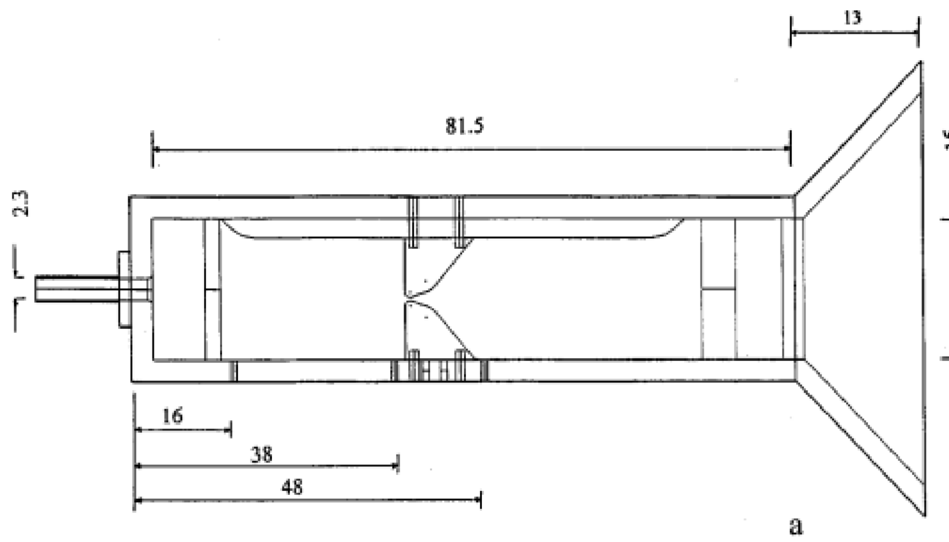

Figure 6: Schematic of the M5 model consisting of wind tunnel, upstream section, vocal folds, downstream section and the exit tubing. Taken from Scherer et al. (2000), cropped.

The vocal folds of the M5 model were attached to wind-tunnel walls by screws and were replaceable, thus allowing usage of vocal folds with different geometries. The vocal fold geometry in the M5 model was enlarged, however the design along with its equations (Figure 7) can, and has been, used with human values successfully in variety of vocal fold models (e.g., Thomson *et al.* 2005, Becker *et al.* 2009).

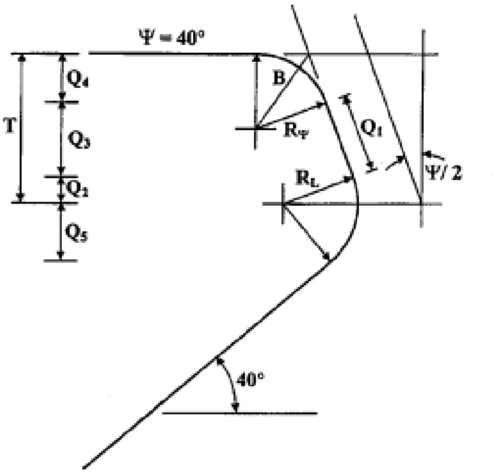

General vocal fold surface design equations :

$R_o = 0.0987$ cm $\quad T = 0.3$ cm $\quad -40° \leq \Psi \leq 40°$

$R_\Psi = R_o / (1 - \sin(\Psi/2)) \quad R_L = R_{40} = T/2$

$B = \sqrt{2}\, R_\Psi / \sqrt{1 + \sin(\Psi/2)}$

$\quad = R_o \sec(\Psi/2) / \sqrt{(1 - \sin(\Psi/2))/2}$

$Q_1 = (T - R_\Psi) \sec(\Psi/2) + (R_\Psi - R_L) \tan(\Psi/2)$

$\quad = (T - R_o - R_L \sin(\Psi/2)) \sec(\Psi/2)$

$Q_2 = R_L \sin(\Psi/2) \quad Q_3 = Q_1 \cos(\Psi/2)$

$Q_4 = R_o \quad Q_5 = R_L \sin 50°$

Figure 7: Schematic design of vocal folds for M5 model and design equations with human values. Taken from Scherer et al. (2011).

2.3.2.2 Externally driven models

Externally driven physical models were developed as the next step to create the model more resembling the behaviour of the real vocal folds. In contrast to static models, where the vocal folds don't move at all, the externally driven models simulate the vibrating movement vocal folds during phonation (Figure 8).

The movement of the vocal folds in externally driven models can either be in phase, where both vocal folds move in sync (e.g., Hyakutake *et al.* 2006), or a phase shift can be introduced (e.g., Kucinschi *et al.* 2006), thus making the vocal folds move out of sync, i.e., asymmetrically.

The simulated movement of the vocal folds in externally driven models opened the possibility to study air flow and air pressure in their relation to vocal fold movement. These models have been used for example to study and visualize air flow (Mongeau *et al.* 1997), to observe unsteady vortex dynamics (Triep *et al.* 2005) or to provide data used in validation of computer models (Kniesburges *et al.* 2011).

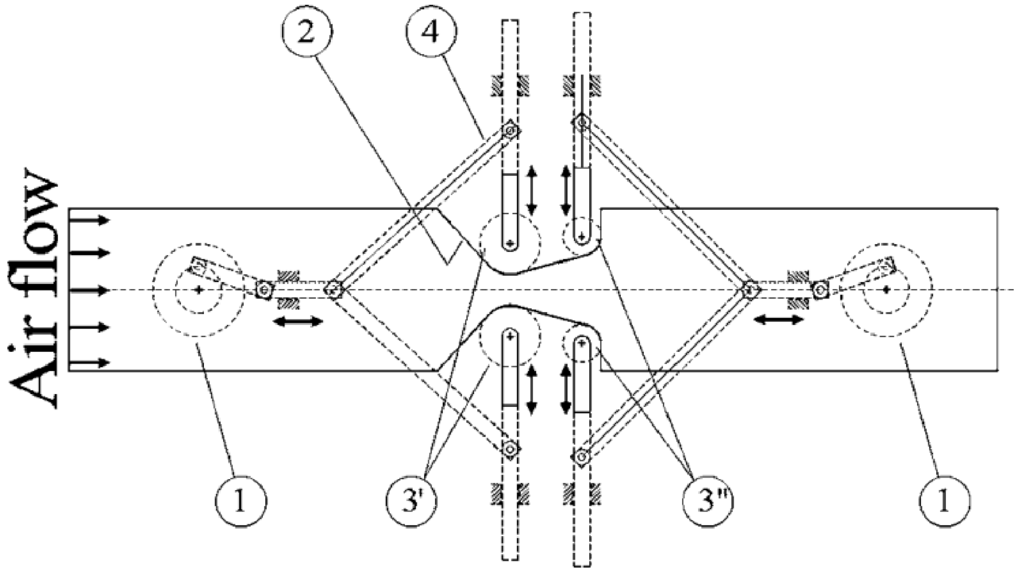

Figure 8: Schematic of the driving mechanism of externally driven models using stepper motors (1), deformable material (2), cylinders (3) and levers (4). Taken from Kucinshi et al. (2006).

2.3.2.3 Self-oscillating models

The static and externally driven models' inability to invoke and study the self-oscillation of the vocal folds severely limited their use. Thus, in the past two decades, researchers focussed on developing physical models capable of self-oscillation.

Currently, the self-oscillating models use synthetic vocal folds from materials with similar properties to real human vocal folds, mainly their elastic properties. In addition to aerodynamics, which can be studied in static and externally driven models, the self-oscillating models can be used to study parameters and phenomena such as phonation threshold pressure or acoustic sound production (Kniesburges *et al.* 2011).

The self-oscillating models can further be divided into three categories roughly corresponding to their chronological emergence. The first category of self-oscillating models uses thin membrane-like materials to simulate the vocal folds. These models were the first models capable of self-oscillation, they used materials such as silicone rubber sheets (Figure 9) to observe high-speed deformations of the vocal fold model and measure threshold pressure (Deguchi *et al.* 2006), two water-filled latex tubes to study and improve physical modelling (Ruty *et al.* 2005) or surgical glove parts to study fundamental frequency of phonation (Kataoka *et al.* 2001). The other two categories of self-oscillating models both use molds to cast the vocal folds elastic materials, the main difference between them being the number of layers used.

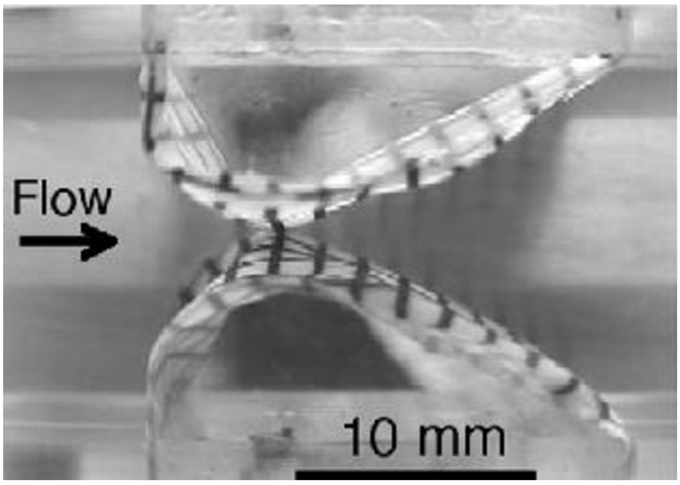

*Figure 9: The membranous-type self-oscillating model using silicone rubber sheets to simulate vocal folds. Taken from Deguchi et al. (*2006).

2.3.2.3.1 Single-layer self-oscillating models

The single-layer self-oscillating models use homogenous vocal folds made of elastic materials, which are poured into molds in the desired shape of the vocal fold, therefore allowing precise geometries to be used as opposed to membrane models.

In his doctorate thesis, Thomson (2004) used a single-layer model made of polyurethane compound (Figure 10) with geometric and material properties similar to human vocal folds, with which he managed to achieve self-oscillation. The vocal folds had Young's modulus of 13.7 kPa, used M5 geometry and self-sustained oscillation was achieved at the frequency of 120 Hz. Thomson discovered that weak surface adhesive forces were responsible for the appearance of a maximum in the frequency-subglottal pressure relation. He concluded that these forces could possibly contribute to damage of the vocal folds in cases, where the laryngeal mucosal lining is dehydrated.

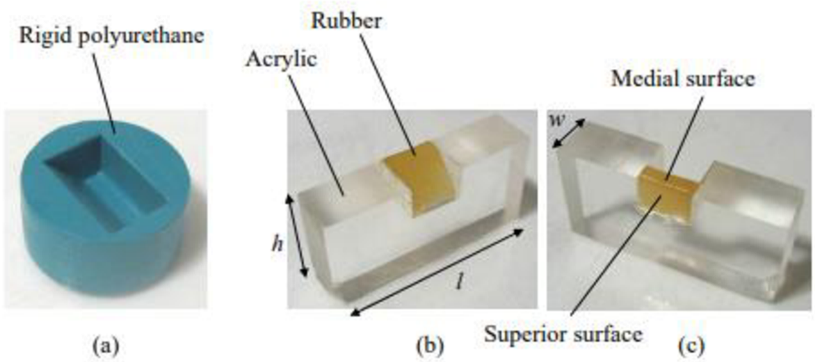

Figure 10: Mold used to cast the vocal folds (a) and views of the vocal fold fixed to acrylic support (b) and (c). Taken from Thomson (2004).

Becker *et al.* (2009) also used single-layer self-oscillating vocal folds made of polymer solution. The vocal folds had Young's modulus of 6,5 kPa and M5 geometry was used. However, these vocal folds vibrated only at very small amplitudes. Researchers alleviated this problem by adding a small mass body cast made of lead into the tip of each vocal fold. The test channel consisted of mass flow controller delivering both constant and pulsating air mass, settling chamber and main testing section, in which the vocal folds were situated. The experiments on the model supported the existence of Coanda effect during phonation with the flow attaching to one vocal fold while separating from the other.

Later, Šidlof *et al.* (2011) used a single-layer vocal folds model made using silicone rubber, however they did not use M5 geometry. The authors decided to make the shape more specific and akin to real larynx and used their own geometry, which they acquired by measuring excised female larynges. To be able to perform high-resolution measurements, authors also decided to scale up the dimensions of the model by the factor of four. Authors used the model to study flow-induced vibrations (Figure 11), specifically flow separation, and concluded, that the separation point remans at the narrowest cross-section during phonation, only moving downstream shortly prior and after glottal closure.

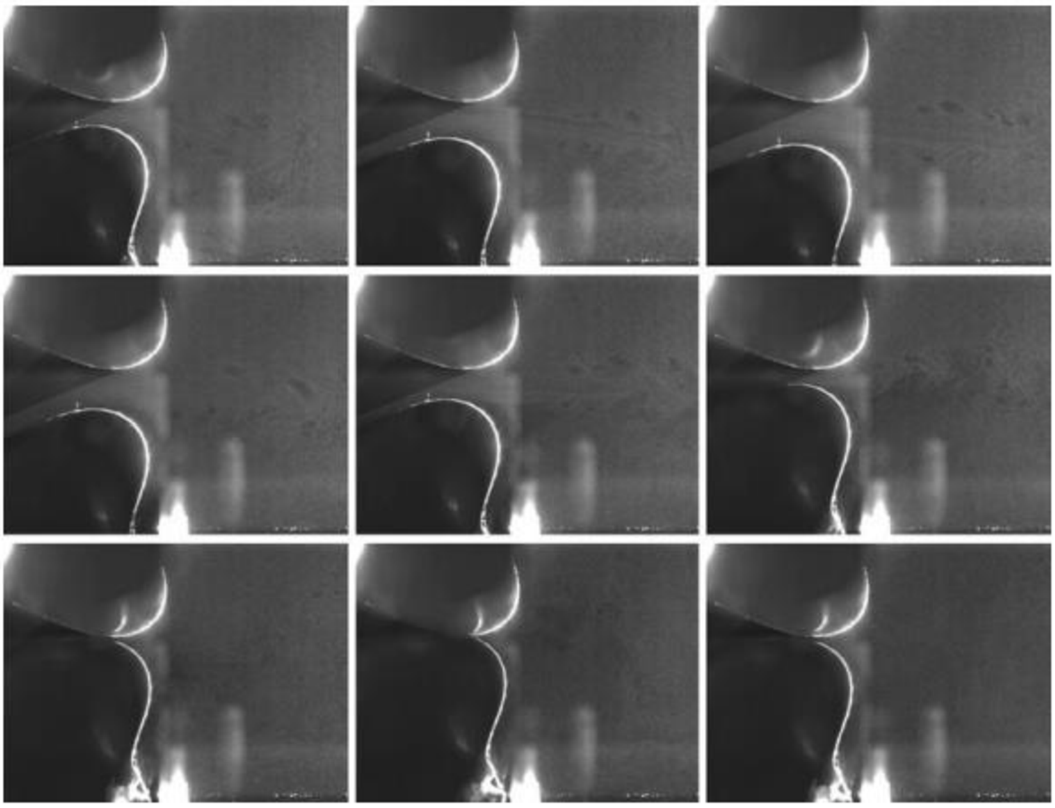

Figure 11: Nine phases of an oscillation cycle in flow induced vibrations of the vocal folds model. Taken from Šidlof et al. (2011).

2.3.2.3.2 Multi-layer self-oscillating models

The multi-layer self-oscillating models use elastic materials for fabrication of the vocal folds similar to single-layer models, however, instead of the vocal folds being made as a single homogenous piece, these models resemble the real vocal folds better by having multiple layers. These models usually either have two layers, body and cover, or three layers, body, ligament and epithelium. The first multi-layer self-oscillating models were two different two-layer models developed by the group of Thomson and published by Riede *et al.* (2008) to study acoustical functions of mammalian air sacs and by Drechsel and Thomson (2008) to study the influence of the vocal tract and false folds on the glottal jet.

Pickup and Thomson (2009) used multiple two-layer synthetic vocal folds in their research to study the influence of asymmetrical vocal folds on voice production. The authors used multiple vocal folds with varying stiffness, the left vocal folds properties were kept constant with Young's moduli for cover being 3.3 kPa and for body being 8.9 kPa. However, the right vocal folds were different to study the asymmetrical influence, with Young´s moduli of the cover being between 2.9 and 8.7 kPa and of the body between 7.8 and 9 kPa. The authors used particle image velocimetry to determine, that the glottal jet was greatly skewed towards the stiffer vocal fold (Figure 12) and listed potential application to clinical conditions.

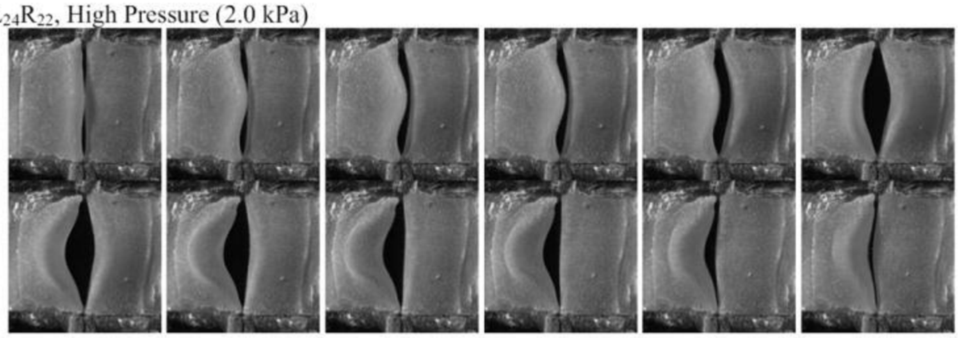

Figure 12: High speed images over one cycle for asymmetric vocal folds. Taken from Pickup and Thomson (2009), cropped.

Weiss *et al.* (2016) used three-layer synthetic vocal folds in their model to aid in development of a collision force sensor. The vocal folds used M5 geometry and were made of a silicone rubber. The three layers used were cover, ligament and body, with Youngs moduli being 3.1 kPa, 70.2 kPa and 10.3 kPa respectively. The vocal folds oscillated with the frequency of 177 Hz which is within the phonatory range, however onset pressure was 3.24 kPa, which is higher than the maximum pressure during human phonation of 3 kPa (Titze and Alipour 2006). The authors analysed the material properties and vibratory behaviour of the synthetic vocal folds using variety of simulation-based techniques and sensors and provided an analytical basis to help improve the understanding of the fluid-structure-acoustic interactions.

Another research study was published by Murray and Thomson (2012) in which they compared four self-oscillating vocal folds with different geometries and number of layers. Of the four different vocal folds, three were two-layer models, two of those used M5 geometry with modifications and the third two-layer model used geometry derived from MRI data. The last model (Figure 13) was designed to overcome the cover stiffness limitation of two-layer models and consisted of four layers, body, ligament, superficial layer of the lamina propria and thin epithelium. The authors performed measurement with these models in full larynx and hemilarynx configurations to determine their possible application in further studies. The last model's frequency, onset pressure and medial surface motion were comparable to human vocal fold data and exhibited mucosal wave-like motion, which plays important part in human vocal fold vibration.

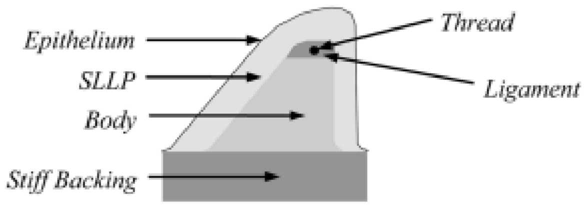

Figure 13: Schematic of multilayer model affixed to stiff backing. Taken from Murray and Thomson (2012), cropped.

A different type of a self-oscillating vocal fold model, developed by a Czech group, contained a silicone cover filled with various materials. Early on the skin was filled with a polyurethane compound (Horáček *et al.* 2008). Later, the vocal fold models' skin was filled with water and silicon wedge was added to act as the vocal folds body, thus creating a three-layer model (etc. Horáček *et al.* 2017 and Horáček *et. al* 2019). The experimental setup for these later models additionally consisted of a model of human lungs with up to fourth-order branching of the airways and a plexiglass vocal tract model beside other basic parts. The vocal folds were in a 1:1 scale with the length of 20 mm, vertical thickness of 10.3 mm and a width of 8 mm. The middle cross-section of the vocal fold was based on computed tomography measurements of a female subject. The filling of the water lowers the frequency of phonation made by the vocal fold model to 80 Hz and the phonation threshold flow reaches even the lowest limits of human phonation. The models were used to study and explore effective mechanisms of voice therapy methods.

In the recent years, researchers focused also on making the vocal fold models conductive, to allow the usage of electroglottography in studying the vocal fold vibrations. Conte *et al.* (2021) developed a three-layered model made of silicone compound using 3D printed molds. The conductivity of the vocal folds was accomplished by a making an additional layer on the surface of the vocal folds, which was made from silicone mixed with a conductive material. The authors declared that this model does not replicate real vocal folds, where the vocal folds are themselves conductive. However, they stated, that for the intentions of their research, which was to monitor vocal folds contacting and decontacting phase, the use of conductive layer was sufficient. The researchers used multiple vocal fold models, with some being made in a shape of healthy vocal folds and some as focal folds with polyps. The vocal fold model showed oscillation similar to human vocal folds and the electrical signals acquired from vocal fold model with an artificial polyp were similar to signal from clinical electroglottography of real human vocal folds with a polyp (Figure 14).

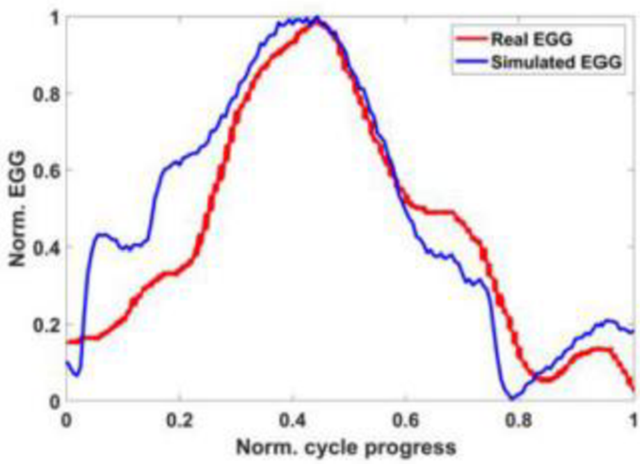

Figure 14: Clinical (red) and simulated (blue) electroglottography signal of vocal folds with polyp. Taken from Cante et al. (2021).

2.3.2.3.3 Fabrication of self-oscillating vocal fold models

The synthetic vocal folds used in self-oscillating models are mostly manufactured by using molds. Several materials, such as polyurethane rubber and silicone compounds are then poured into the molds, once the material hardens, the vocal folds are affixed to backings and used.

Becker *et al.* (2009) used a single-layer self-oscillating vocal folds in their research, which focused on existence of Coanda effect during phonation. The authors manufactured the vocal folds by casting polyurethane solution into molds. The stiffness of the vocal folds was determined by mixing ratio of the different compounds of the solution. The vocal folds were then fitted with small mass body cast into each tip to increase amplitudes of vibration. Manufacturing of most of the single-layer model usually consists of the same steps, where the material solution is poured into a mold with the mixing ratios needed to achieve the desired properties, thus creating a homogenous vocal fold model.

Murray and Thomson (2011) published an article solely focused on fabrication of multi-layer self-oscillating vocal fold model. The molds for superficial lamina propria, ligament and body layers were created by making computational 3D models, exporting them as STL files and then sending them to a custom machine shop to be manufactured (Figure 15).

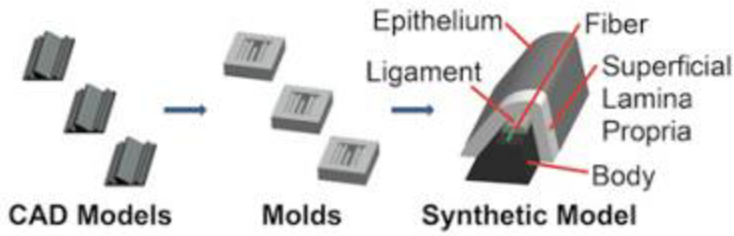

Figure 15: CAD models (left), manufactured molds (middle) for each layer and synthetic multi-layer vocal fold model (right). Taken from Murray and Thomson (2011).

Release agent was applied into the molds to help in separation of silicon from the molds once it hardened. The silicone compounds A and B were mixed with a thinning agent in 1:1:1 ratio respectively to achieve the desired properties of the body layer. The mixed solution was then placed in a vacuum chamber to remove air from the material; afterwards the solution was poured into the mold and placed in oven. The backing of the model was then made by pouring silicone and thinning agent solution of the same ratio as before into the body mold and once again placed in vacuum chamber and subsequently in the oven, thus creating a joined body-backing part of the model. The solution for the ligament layer was prepared with 1:1:4 ratio and poured into its mold in the same way. The body-backing part of the model was then pressed into the ligament mold and placed into the oven resulting in a combined ligament-body-backing part. Superficial Lamina Propria layer was made and combined into one part with the previous layers in the same way as the ligament layer. Finally, the solution for the epithelium layer was mixed, placed into the vacuum chamber, poured onto the combined part, and allowed to cure. Once both vocal folds were fabricated, they were mounted into acrylic mounting plates using a silicone glue. By using screws, the mounting plates were brought together in a fashion similar to human vocal folds (Figure 16). The authors also created a video of the fabrication process as a supplement to the article, which shows the entire process of fabrication.

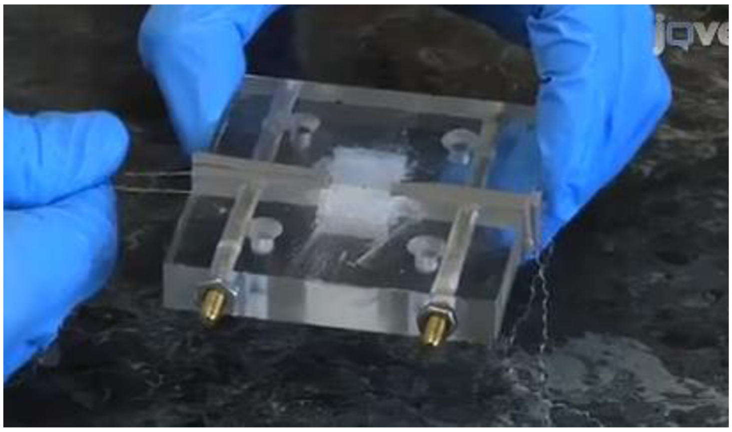

Figure 16: Stilt form the video of multi-layer vocal fold model fabrication, showing the vocal folds mounted in the acrylic mounting plated and fixed together using screws. Taken from Murray and Thomson (2011).

In a recent article, Birkholtz *et al.* (2019) used a three-layered vocal fold model, which they manufactured in a different fashion compared to other authors. An aluminium frame for the vocal fold was milled in a workshop and CAD models of negatives for each layer were then designed and manufactured by a 3D printer using water-soluble material. The body layer negative was then glued to the frame forming a mold (Figure 17). The body-layer solution was poured into the mold seeping into the open spaces in the walls of the aluminium frame, thus fixing the vocal fold to frame. Once the solution cured, the negative was dissolved in water and the cover layer negative was glued to the frame. Silicone solution for the cover layer was then poured into the mold, left to cure and then the negative was once again dissolved in water. The epithelium layer was created by slowly pouring the epithelium silicone solution over the cover layer; most of the liquid silicone drained away and only a thin film adhered to the cover layer.

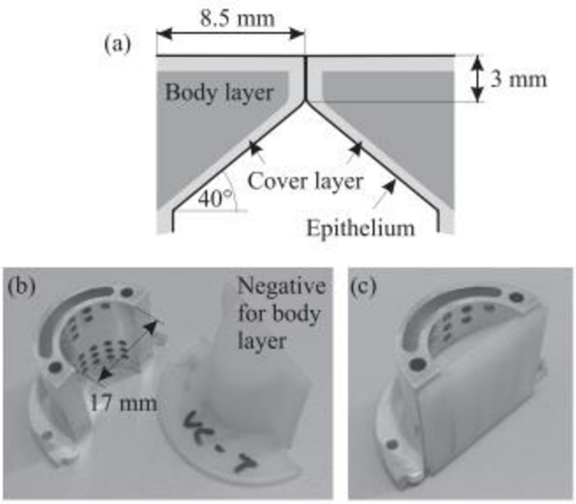

Figure 17: Central coronal cross-section through the silicone layer (a), the aluminium frame and the negative (b) and the frame and the negative glued together (c) used in fabrication of three-layer self-oscillating vocal fold model. Taken from Birkholtz et al. (2019).

Fabrication of conductive single-layer self-oscillating vocal fold model was described by Syndergaard and Thomson (2017). The vocal fold model used M5 geometry, and its single layer was made from silicone parts A and B and silicone thinner solution with 1:1:4 ratio. The outside surface of each vocal fold replica was coated with graphite powder until it was visibly covered to add the conductivity to the model. Each vocal fold replica was then mounted to an acrylic plate. The authors attempted to mix the graphite with the silicone solution, however they found out, that the amount of particles required to achieve conductivity resulted in the material properties to be altered in such a way, that flow-induced vibrations were no longer possible. The authors used the model to present a method of monitoring the vibrations of the vocal fold models using resistance measurements.

3. AIM OF THE THESIS

The aims of this thesis were to develop a supporting framework and a single-layer vocal fold model to be used in studies of phonation. The supporting framework was to be made compatible with previously developed and manufactured parts of the experimental setup. Main goals for the supporting framework were to feature important functions present in human phonation, such as the ability of abduction and adduction, variability of the inner tension of the vocal folds and left-right symmetry or asymmetry and to be highly modular. Another aim of this thesis was to serve as a manual of the fabrication process for the vocal fold models, that could be used in future studies. The last goal was to test the manufactured silicone models for their ability of self-oscillation.

4. MATERIAL AND METHODS

4.1 Experimental setup

The experimental setup´s subglottal part consisted of an air pump, acting as artificial lungs, and an artificial trachea, both of which were developed and manufactured in the Voice Research Lab for the purpose of excised larynx experiments before the work on this thesis began. This thesis focused on developing a supporting framework for the vocal fold model with space and plans prepared to manufacture and add artificial vocal tract. The entire experimental setup can be seen in (Figure 18).

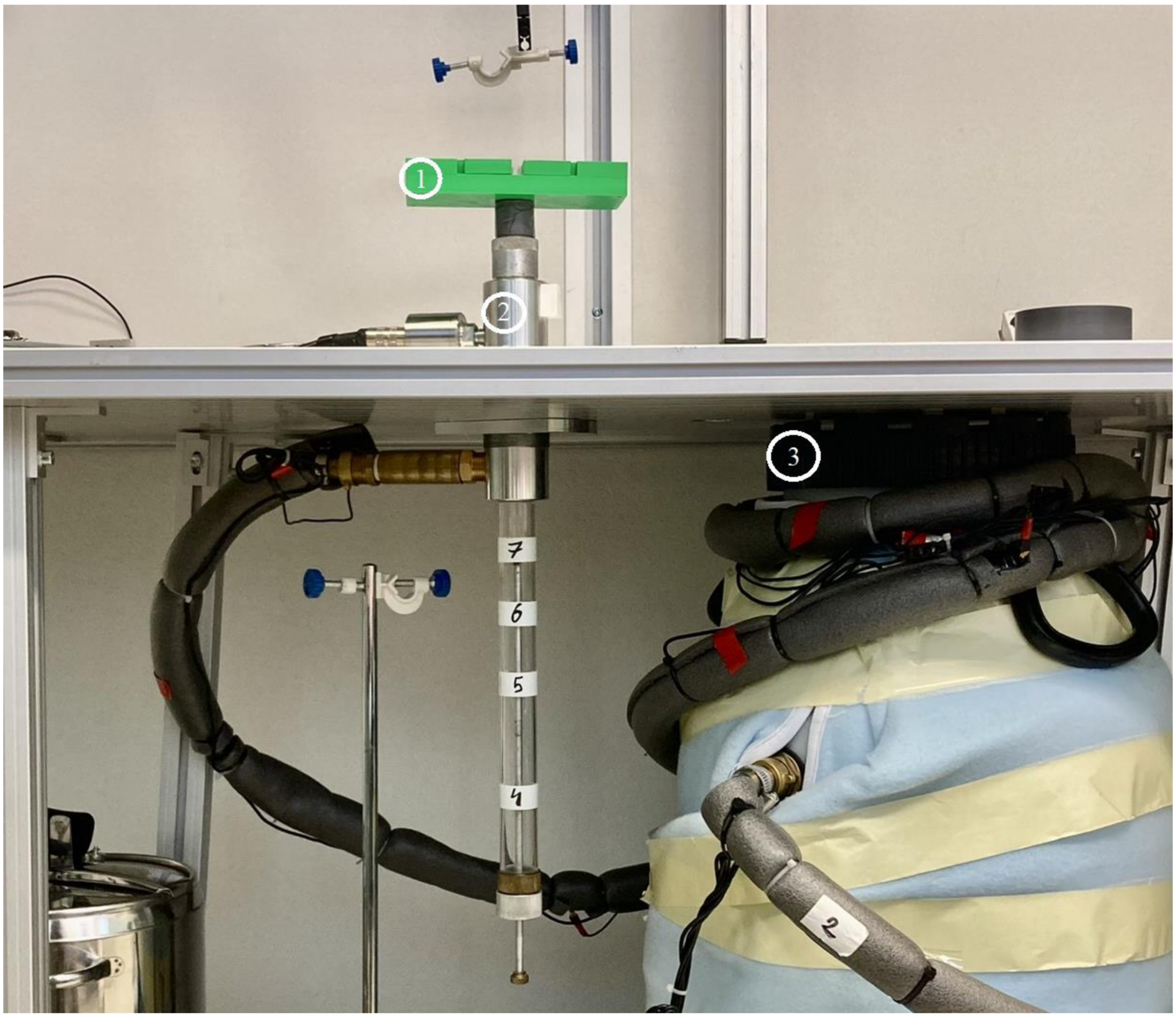

Figure 18: The experimental setup containing the supporting framework for the silicone vocal folds (1), artificial trachea (2) and artificial lungs (3).

Airflow for the vocal fold oscillation was provided by an air pump (RESUN LP 100) connected to the artificial trachea. The artificial trachea (Figure 19) was developed and manufactured before the work on this thesis began, it´s design was based on a utility model of Hampala *et al.* (2013) with some alterations made primarily by Ing. Petr Hájek, Ph.D. The artificial trachea featured openings for laryngoscope and pressure sensor, an entrance for pressurized air and many other features. The details of the artificial trachea can be accessed from Ing. Petr Hájek, Ph.D. personally.

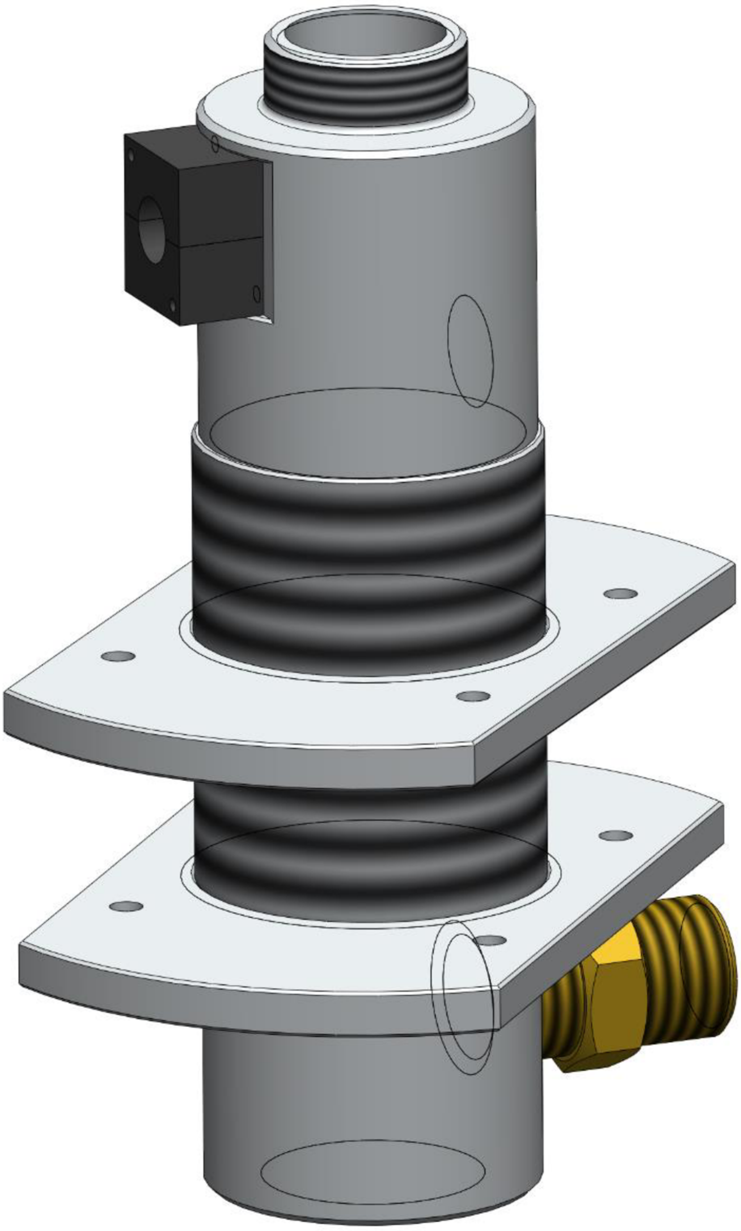

Figure 19: The model of the artificial trachea used in the experimental setup.

4.1.1 3D modelling

The parts used in this thesis were 3D modelled using Autodesk Inventor, a software commonly used to model 3D objects, by the company Autodesk, Inc. For parts, which were 3D printed, the models were exported as STL files using a built-in function of the Autodesk Inventor software.

4.2 Vocal fold model

This thesis used single-layer vocal fold models to study the phonation. The single-layer vocal fold models were used for the developments phase because of their relative simplicity and ease of manufacturing as opposed to more complex models, which might be used once the supporting framework is proven to be functional. The vocal fold model´s geometry (Figure 20) was based on M5 geometry proposed by Scherer *et al.* (2001) and the parameters were set so that the vocal folds had physiologically realistic dimensions. The descriptions of each parameter and the equations can be found in Figure 7 in the theory part of this thesis. The M5 geometry was later used to 3D model and print a mold used for casting of the vocal fold models.

M5 geometry – parameters:

R_0 = 0,987 mm, T = 3 mm, Ψ = 5°

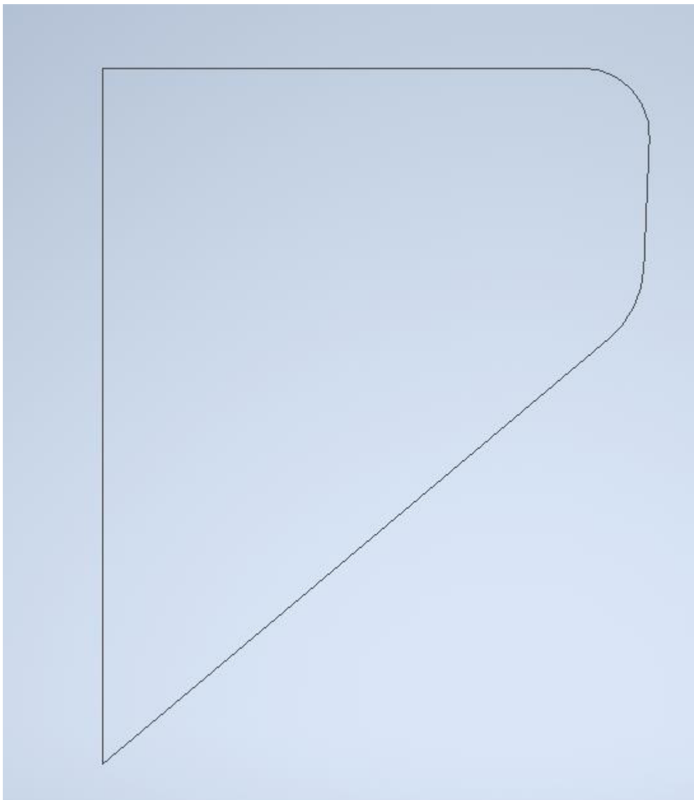

Figure 20: The M5 geometry modelled in Autodesk Inventor used to obtain the molds for artificial vocal folds.

4.2.1 Materials for the vocal fold model

To fabricate the vocal folds, two silicone compounds was used. The first silicone used was Ecoflex 00-10 from the company Smooth-on, Inc. The manufacturer specified the Young´s modulus value of 60 kPa and the viscosity of 14 000 mPa·s. Later, Ecoflex 00-10 was mixed with Silicone Thinner, again from the company Smooth-on, Inc., which is a product that lowers the silicones viscosity and elasticity. Several mixing ratios were used.

The second silicone compound used was Ecoflex 00-30 for which the manufacturer specified the Young´s modulus of 70 kPa and the viscosity of 3000 mPa·s. Ecoflex 00-30 was again mixed with Silicone Thinner in several different ratios.

As part of this thesis, measurements were performed to determine the Young´s moduli of certain silicone compounds used. The measurements to determine the Young´s moduli of used silicone compounds were performed in the Institute of Solid Mechanics, Mechatronics and Biomechanics, Faculty of Mechanical Engineering, Brno University of Technology by Ing. Anna Hrubanová. To measure the Young´s moduli of the compounds, a precise sample with dimensions of 20×20×1 mm had to be made for each of the compounds. To make these samples, a mold was 3D modelled and printed (Figure 21) and the samples were cast the same way as the vocal folds (the step-by-step instructions are provided in the next part).

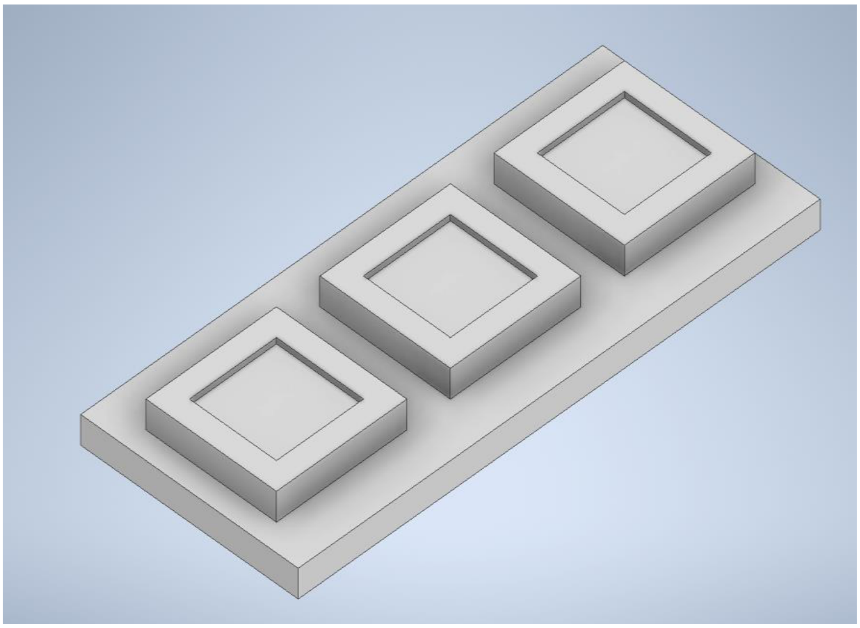

Figure 21: 3D model of a mold used for casting the silicone samples for testing purposes.

The equibiaxial tests of the samples were performed and strains were obtained through DIC reading. Stresses in each in-plane direction were captured by gauge heads and calculated from recorded forces and cros-section of the unloaded samples (Figure 22).

Figure 22: The testing device used to determine the Young´s moduli of silicone compounds used in the thesis.

4.2.2 Fabrication of the vocal fold model

The fabrication process of the vocal fold model began with the 3D modelling and 3D printing of the mold (Figure 23) using the M5 geometry. Once the mold was printed, the excess material left over from the 3D printing had to be removed using sandpaper and files.

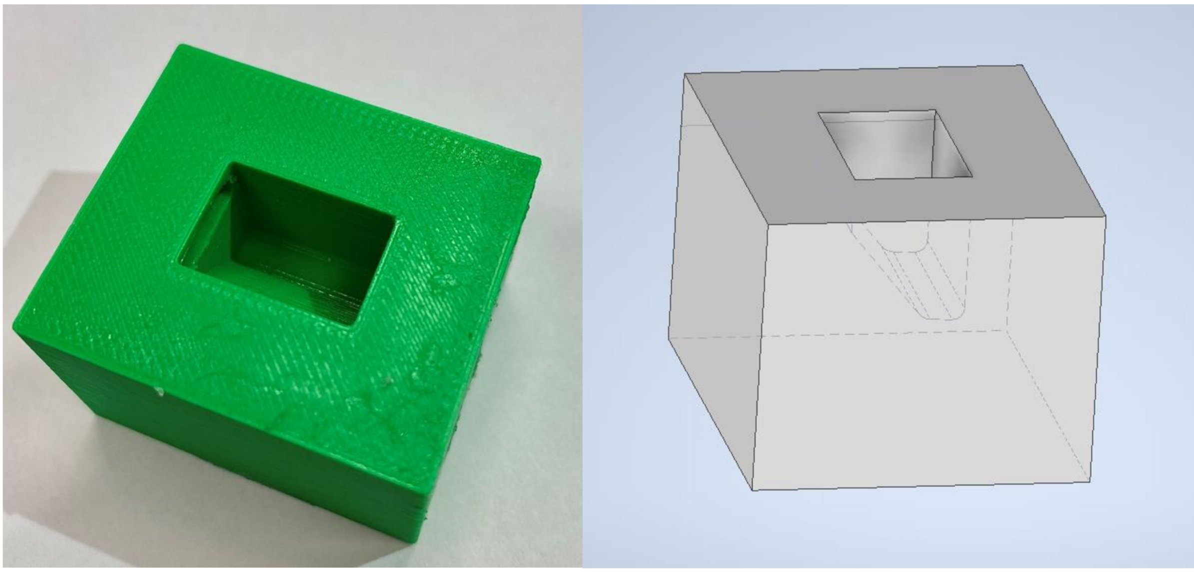

Figure 23: The 3D printed mold used to cast the vocal fold model from silicone compounds (Left) and its 3D model made in Autodesk Inventor (Right).

Once the mold was prepared, the silicone compound of the decided ratio was mixed in a beaker. The individual parts of the compound were added using syringes to ensure that all parts of the compound were in correct volumes. The compound was then mixed for 5 minutes using glass rod until all the parts were mixed thoroughly. The beaker containing the compound was placed into a vacuum chamber (Figure 24) to remove air bubbles, which could influence the properties of the vocal fold.

Figure 24: Vacuum chamber used to remove air from the silicone compounds.

The molds were set on an even surface and a small amount of a silicone separator was added using a brush to help with the removal of the vocal fold once the silicone hardened. The silicone compound was poured inside until the mold was slightly overflowing, the excess compound was swiped with flat piece of plastic to ensure, that the vocal fold had the correct dimensions. The silicone was then left to cure for at least 8 hours.

Once the silicone had cured, the vocal fold was carefully removed from the mold to ensure that no damage was made to it. In the simplified prototype used in testing the model before final fabrication, the vocal folds were then glued straight into a space in the supporting framework.

In the non-simplified final version of the supporting framework, the vocal fold model was cast with a hole for a bar (Figure 25 a), which was designed to allow the vocal fold model to freely slide along it to provide more realistic boundary conditions during model stretching/elongation than the ones present with vocal fold model glued to the supporting framework directly. Once the vocal fold model´s silicone cured, the bar was inserted into the hole in the vocal fold model. Using the bar, the vocal fold model was inserted between L-shaped parts of the supporting framework responsible for stretching and pressing the vocal fold model (Figure 25 b). The vocal fold model was then glued to the L-shaped parts in a careful way, to prevent the bar itself to be glued to the L-shaped parts.

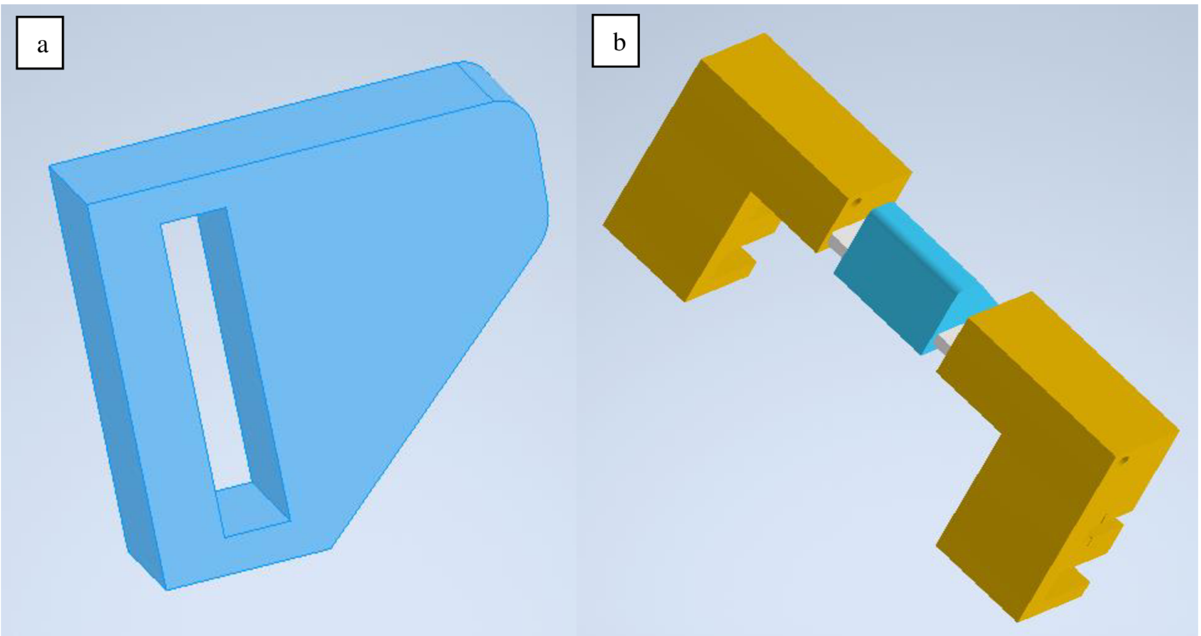

Figure 25: 3D virtual model of the vocal fold model with the hole for the bar visible (a) and virtual model of the vocal fold model with the bar inserted inside it and the L-shaped parts (b).

4.2.3 Measurements of the phonation parameters

During the testing of the vocal fold models, several parameters important in phonation were measured to determine the functionality and quality of the vocal fold models. The first parameter measured was the subglottal pressure, which was measured using the DC pressure sensor (KELLER PR-41X).

The second parameter measured was the fundamental frequency of the vocal fold model´s phonation, this was done by obtaining the signal using the microphone (MicW M416) at the distance of 14 cm and the Praat software developed by Paul Boersma and David Weenink (2013).

Last parameter measured was the airflow coming from the air pump, which was measured using the flow meter (DF 4.01K5 by Emkometer) and the flow head (GM Instruments, F300L).

The signals were captured and digitized using an 8-channel digital acquisition system (Dewetron DEWE 43 V). All the parameters were then processed using the software DewesoftX (by the DEWESoft company). Several screenshots from videos of the self-oscillating vocal fold models were made. The videos were recorded using a smartphone camera. To be able to record the vocal fold models during oscillation, a stroboscope (ELMED Helio-Strob micro2) had to be used. The same stroboscope was also used to approximately determine the frequency of the oscillation.

5. RESULTS

5.1 Supporting framework

5.1.1 Development of the supporting framework

The development of the supporting framework was done using Autodesk Inventor ® software creating virtual models. The early models were simple, with additional features being added and problems corrected, until final version was modelled and manufactured. The first versions (Figure 26) featured the ability of abduction and adduction, i.e., the opening and closing of the glottis.

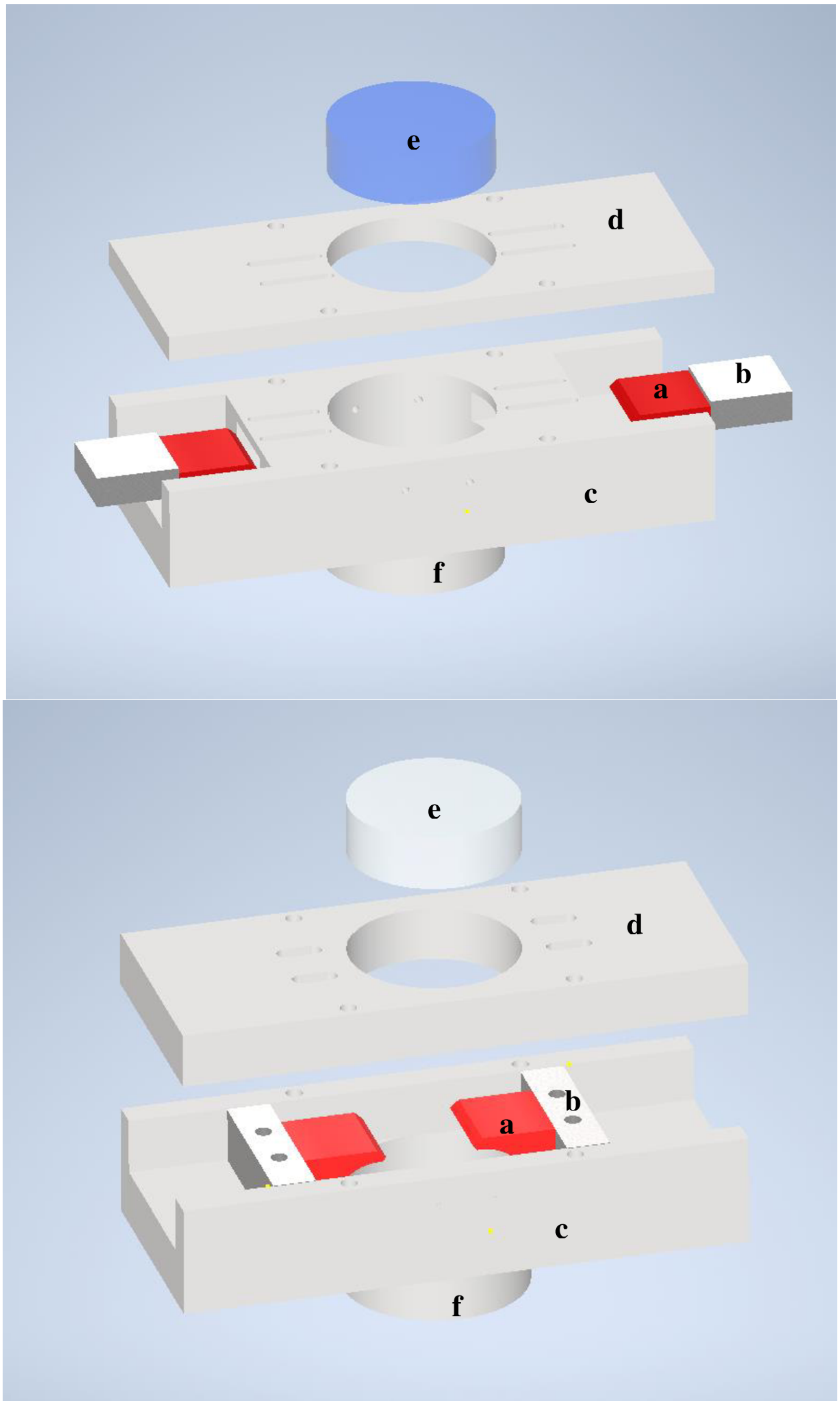

Figure 26: The first and second versions of the supporting framework with simplified vocal fold model (a), bases for the vocal fold model (b), bottom part (c), top part(d), glass closing part (e) and the connecting chamber to artificial trachea (f).

In the first and second versions, the artificial vocal folds (a) were planned to be glued to their bases (b), which would be placed on the bottom part (c) of the supporting framework. The bases could then be moved towards or away from each other, simulating the abduction and adduction of the real vocal folds. Once the vocal folds would be placed at the desired distance from each other, the top (d) of the supporting framework would be placed on top of the bases, connected to the bottom part and the bases would be fixed in their position using screws to prevent them from moving during the experiment. The early versions also included a connecting chamber (f) with screw thread at the bottom to connect the artificial trachea with the model and a glass part (e) used to close the model from the top. The main problems of these versions, apart from featuring only the basic functions, was insufficient insulation of the model, which could result in air leakage and low air pressure acting on the vocal fold model.

Third version was made to fix the problem of the insulation (Figure 27). This version not only fixed the insulation problem, but it also added additional modularity, which was one of the main aims of the thesis, enabling to easily replace parts of the model. This version again featured the ability to simulate abduction and adduction, same as the earlier versions.

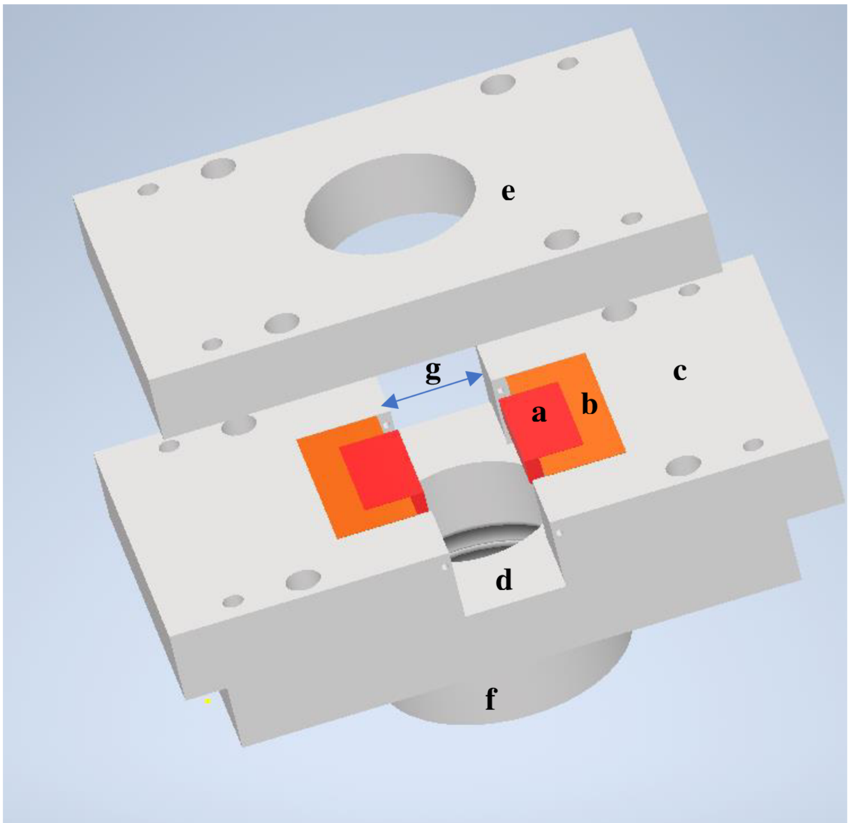

Figure 27: Third virtual version of the artificial larynx with the vocal fold model (a), bases for the vocal fold model (b), middle parts (c) bottom part (d), top part (e) and connecting chamber for the artificial trachea (f).

In the third version, the silicone vocal folds (a) would first be glued to the bases (b) made by 3D printing, thus decreasing the cost for each pair of the vocal folds and allowing to easily replace the vocal fold model. The bases would then be glued into their location in the middle parts (c) of the supporting framework. The middle parts would be placed on the bottom part (d) and moved into the position at the desired distance of the vocal folds. The top part (e) would be placed on top of the middle parts, and the parts would be joined using screws, preventing them from moving during the experiment. During the experiments, holes would be present between the middle parts if the vocal folds would not be touching directly, which can be seen in (g), in these cases, silicone cubes would be placed in the resulting holes to ensure air insulation of the model. This version, like earlier versions, featured a connecting chamber for the artificial trachea with screw thread (f) and glass lid on the top to close the model.

The fourth, last non-final version of the supporting framework was made with a goal to add additional features apart from the abduction and the adduction and to increase the modularity of the model (Figure 28). This version featured the ability to stretch or press (i.e., shorten or elongate) the individual vocal fold, which results in changes of inner tension and plays an important role in phonation.

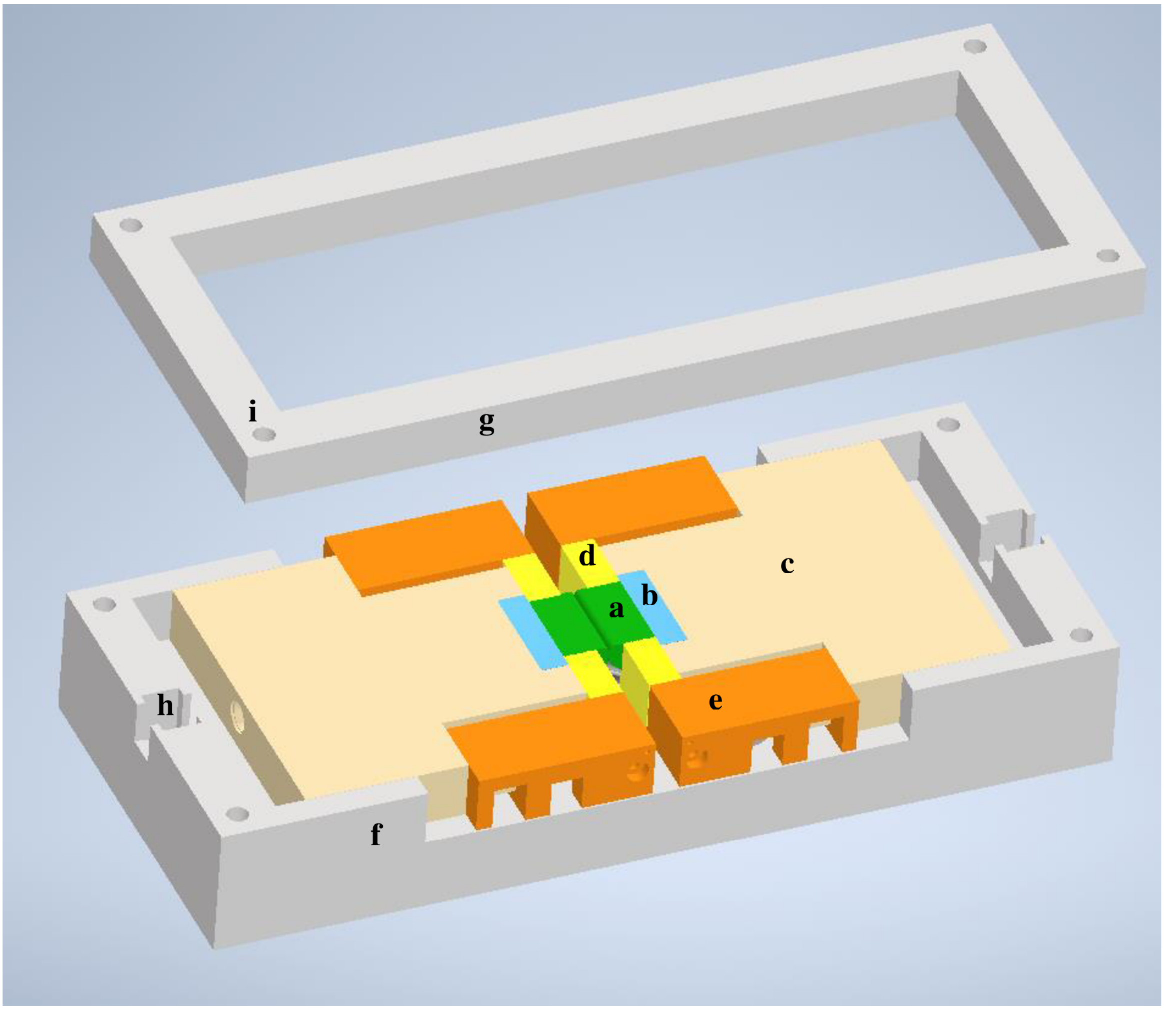

Figure 28: Fourth version of the supporting framework with the vocal fold model (a), bases for the model (b), the middle part (c), the fixing cubes (d), the stretching-pressing part (e), the bottom part (f) and the top part (g).

In this version of the artificial larynx, the vocal fold model (a) would be cast with additional material on the back in a specific shape, which would be used to slide into a groove in its base (b) (Figure 29). This addition would allow the vocal folds to be elongated or shortened along its entire length, as the vocal fold model would slide inside of the groove. In versions, where the vocal fold model was glued to its base, the glued part of the vocal fold model would not be able to be elongated or shortened, making the boundary conditions much less realistic.

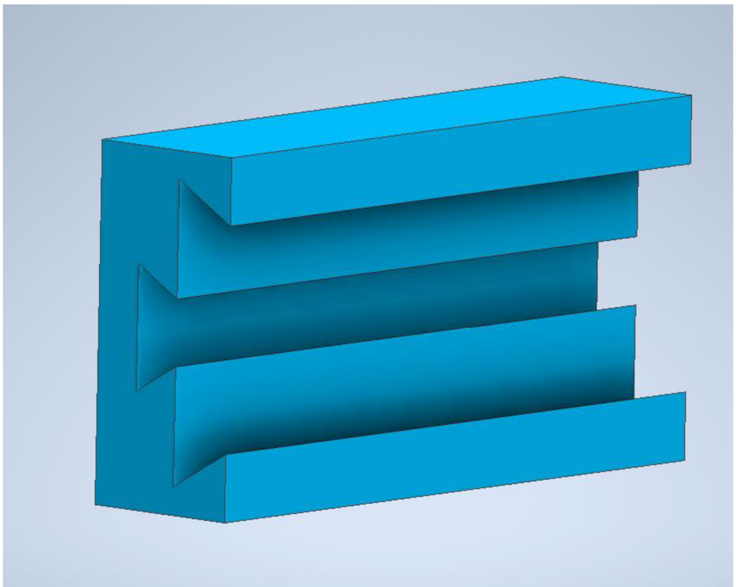

Figure 29: The base of the vocal fold model with a groove for the silicone material on the back of the vocal fold model. In the final version of the supporting framework, a bar replaced this base.

The base would then be glued to their position in the middle part (c) and the cubes (d) would be glued to the vocal folds on their sides, resulting in the vocal folds to be fixed an all sides expect for the sides facing each other. The cubes would be joined with their corresponding stretching-pressing parts (e) by screws. The stretching-pressing parts would then be connected with the middle parts using screws. The screwing or unscrewing of the screws would then move the stretching-pressing parts either toward or away from the middle part, which would result in the vocal fold model being either elongated or shortened. The middle parts would then be fixed to the bottom part (f) with screws on their back sides (h), these screws would allow the middle parts to be moved either away or to each other, simulating the abduction and adduction of the vocal folds. Once the vocal folds would be in the desired distance from each other and would be elongated or stretched as desired, the top part (g) of the model would be placed on the rest of the supporting framework and the entire model would be affixed with screws going through the holes in the corners (i).

The last to final model showed great promise, however, during testing, it was found, that the silicone could not be shaped in correct shape of the groove in its base, resulting in the vocal fold model to not fit inside of the groove. Thus, the final model was developed to fix this issue.

5.1.2 Final version of the supporting framework

The final version of the supporting framework contained the desired features of the previous versions and improved upon them; it also fixed the main issue of the last version, the base of the vocal fold model (Figure 30). The supporting framework consisted of six parts – the bottom part, the top part, the middle part, the bar, the stretching-pressing parts and the connector to the artificial trachea.

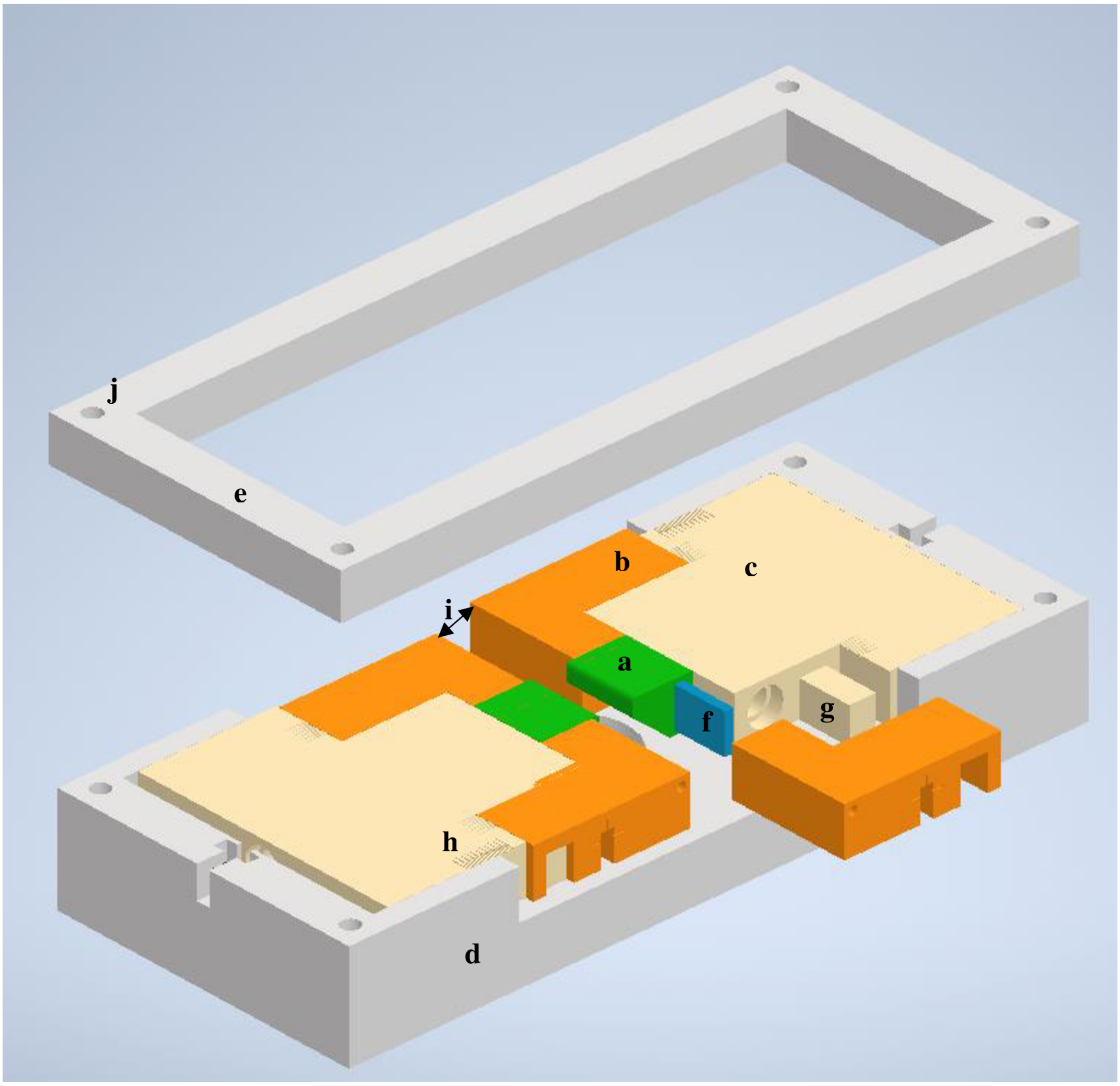

Figure 30: The final version of the supporting framework with the vocal fold model (a), the stretching-pressing parts (b), the middle parts (c), the bottom part (d), the top part (e) and the bar (f).

In the final version of the supporting framework, a bar (f) was first inserted into the vocal folds (a) and the vocal folds were glued to the stretching-pressing parts (b) on their sides without the bar itself being glued to the stretching-pressing parts (the details of the preparation of the vocal fold model, the insertion of the bar and the gluing to the stretching-pressing parts are provided in the Material and Methods section). The stretching-pressing parts were then placed on protrusions (g) in the middle parts (c) to ensure their stability and correct position of them and the vocal fold model itself. The scales (h) were inserted on the surface middle parts and precise screws were then used to position the stretching-pressing parts into neutral position, i.e., the position, where the vocal folds were neither stretched nor elongated. Once the stretching-pressing parts were set in the neutral position, the same screws and scales were used to elongate or shorten the vocal folds based on the parameters of the experiment. The middle parts were then placed on the bottom part (d) and using precise screws and scales again, they were moved to neutral position, where the vocal folds would be touching, but not pressing against each other. Once the middle parts were set in the neutral position, the same screws and scales could then be used to move the two vocal folds away or towards each other, simulating the abduction and the adduction. Once the vocal folds were in the correct position based and elongated or shortened correctly, the holes between the stretching-pressing parts (i) were filled with silicone cubes to ensure air insulation. The top part (e) was placed on the model and the model was joined together using screws through prepared holes (j).

5.1.2.1 Parts of the supporting framework and their functions

The bottom part´s (Figure 31) main function was to provide the base for the other parts and to secure the connection to the artificial trachea.

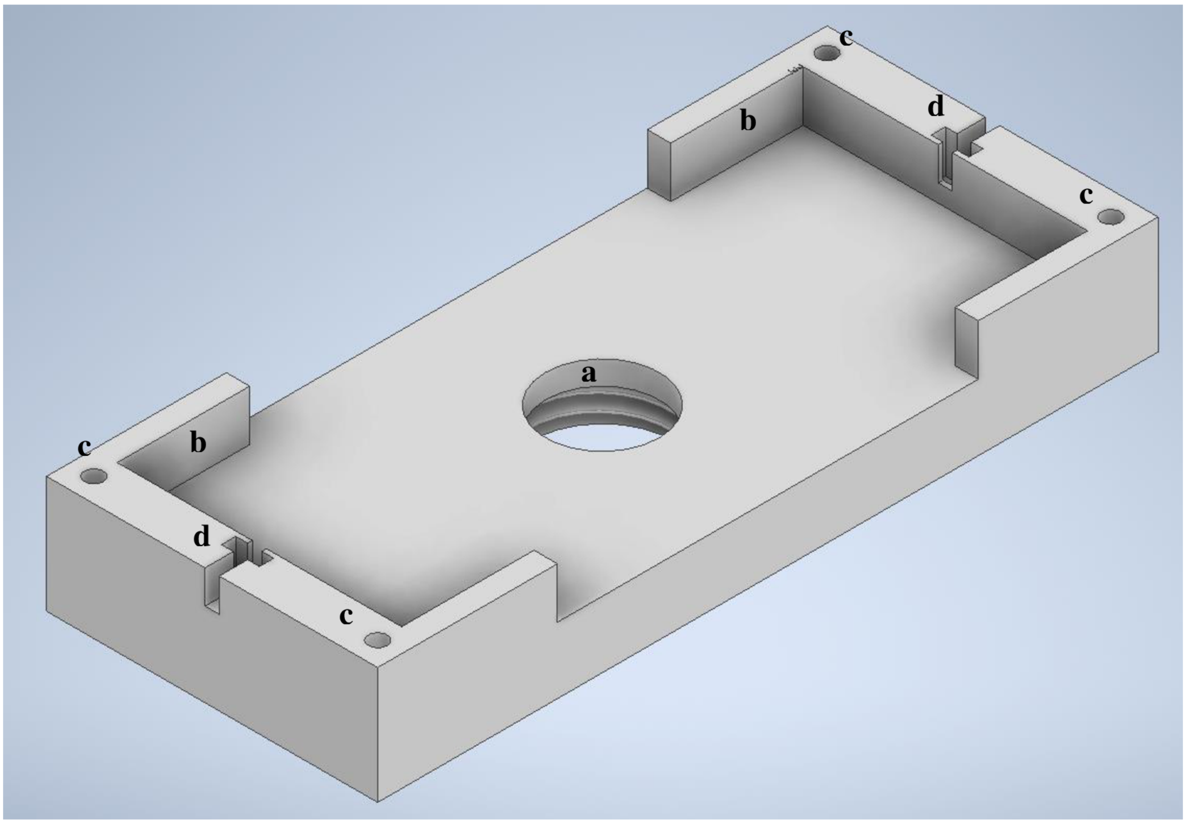

Figure 31: The virtual model of the bottom part of the supporting framework.

In the middle of the bottom part, a hole with a screw thread for the connector for the artificial trachea was placed (a). Parts of the sides of the bottom part were lifted (b) to make a base in which the middle part could move in medial-lateral direction. In the lifted part´s corners, holes were made for screws (c) used to join the entire supporting framework together. The final feature of the bottom part is the holes for the heads of the precise screws (d) used to control the abduction and the adduction of the vocal fold model.

The connector for the artificial trachea (Figure 32) was designed in a way to fit both the artificial trachea and the bottom part of the artificial larynx. Its main function was to lift the supporting framework higher above the artificial trachea so that the position of the silicone vocal folds corresponds to the position of real vocal folds in excised larynx – see e.g., Herbst *et al.* (2017), Lehoux *et al.* (2021).

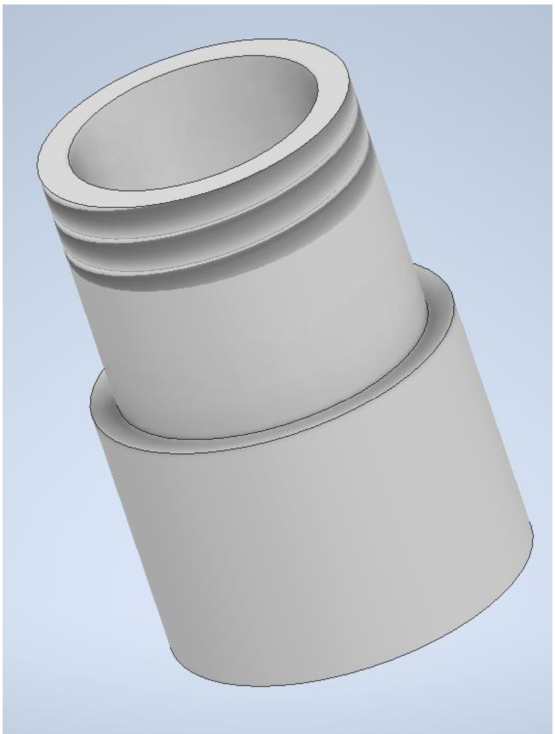

Figure 32: The connector for the artificial trachea.

The middle parts main functions are to ensure the precise abduction and adduction of the silicone vocal folds and to support and hold the stretching-pressing parts (Figure 33).

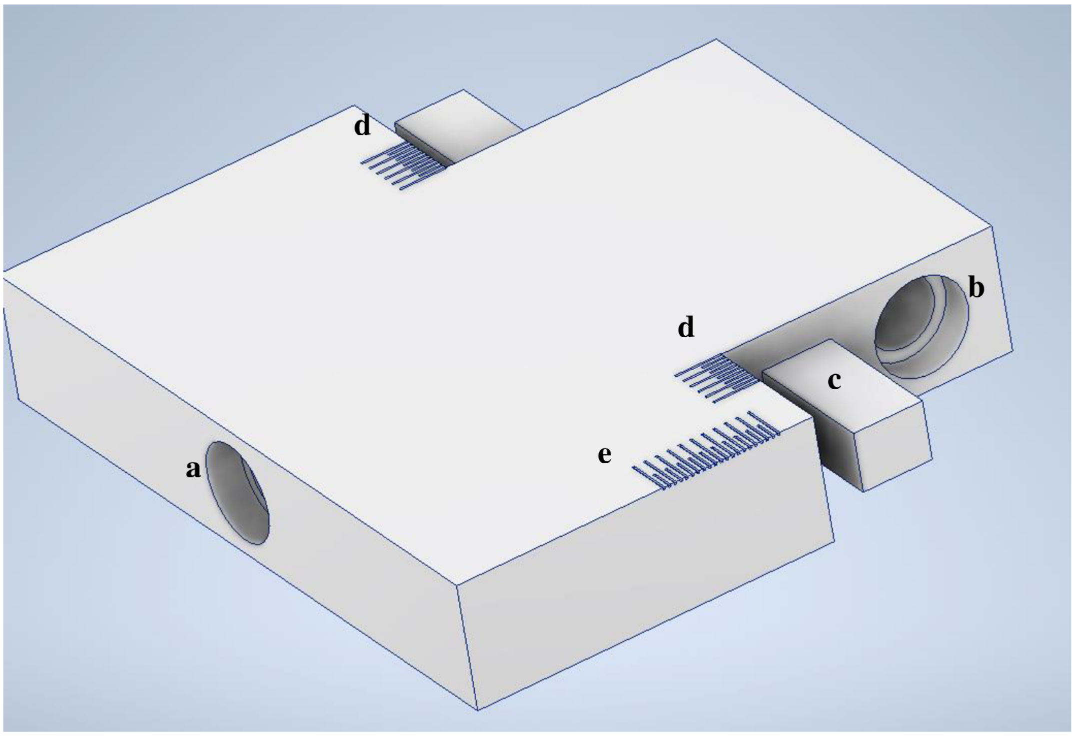

Figure 33: The middle part of the supporting framework.

The middle part featured holes on its back (a) and on its sides (b) for the nuts of the precise screws. The back hole was designed to hold the nut for the precise screw, which's head was placed in its holder in the lifted sides of the bottom part (Figure 31 – d) and which's function was to ensure precise abduction and adduction of the vocal fold model by the movement of the middle part. The side holes were designed to hold the nuts of the precise screws which's head was in the stretching-pressing parts (Figure 34 – b and Figure 30 - b). Additionally, the middle part contained a protrusion (c) on both sides, on which the stretching-pressing part was placed to ensure its correct position in relation to the other parts. Last feature of the middle part was three scales, the dual scales used for the stretching-pressing parts (d) and the scale for the middle parts movement itself (e).

The stretching-pressing part´s functions was to hold, and elongate or shorten the silicone vocal folds (Figure 34). Two types of the stretching-pressing parts were made for the model, resulting in four stretching-pressing parts in the model total. The two types were identical apart from the symmetrical changes.

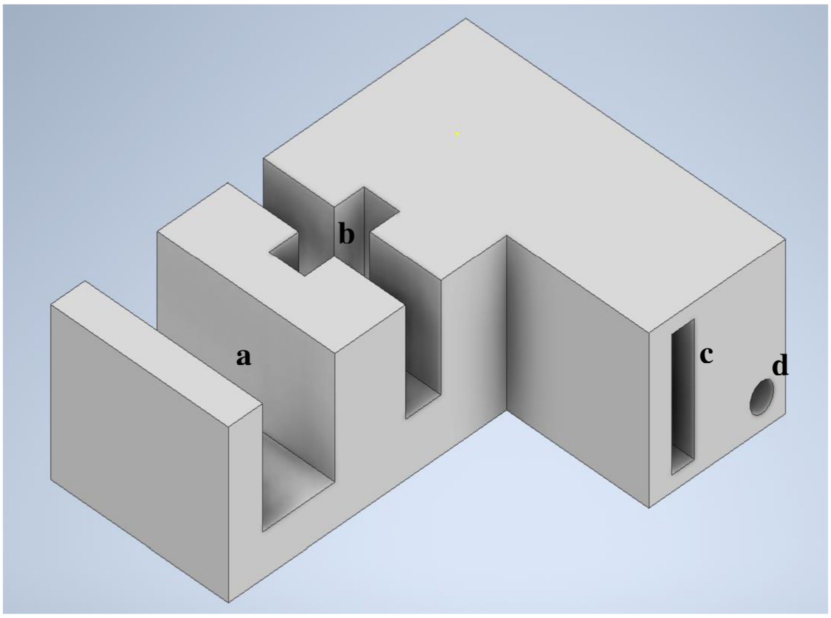

Figure 34: The stretching pressing part of the artificial larynx.

The stretching-pressing parts featured a groove (a) for the protrusion located on the middle part (Figure 33 – c) of the supporting framework, to ensure correct position of this part, hole for the head of the precise screw (b), which was used to ensure precise stretching or pressing of the vocal fold model. Additional features of this part were: the hole (c) for the bar which was inserted into the silicone vocal fold and a circular hole (d) for optional usage of either a water filled vocal folds or a string to simulate the ligament in the vocal fold model in future.

The bar (Figure 35) was designed to fix the problems of the previous versions of the supporting framework, i.e., the gluing of the vocal folds to the bases in earlier versions and the bases with grooves in previous version. Gluing the vocal folds to their bases causes problems for isotonic elongation and shortening of the vocal folds. In the version with grooves in the bases, the silicone could not be made into the correct shape to fit into the groove and would tear itself.

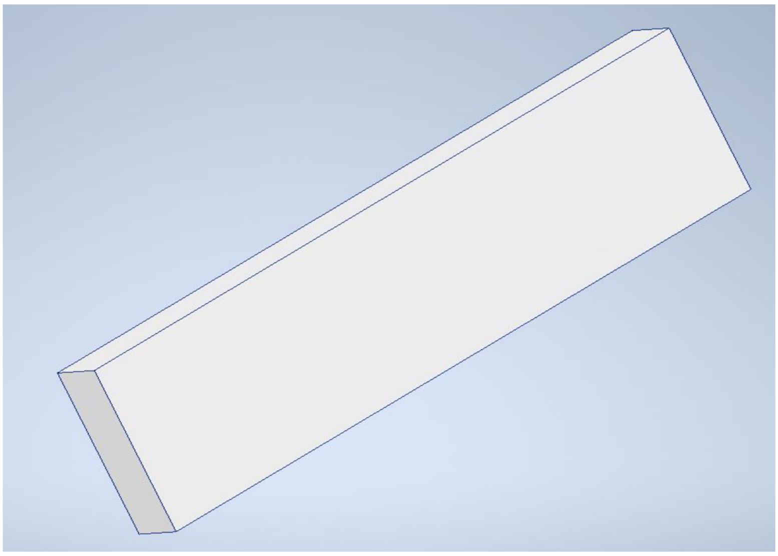

Figure 35: The bar used in the artificial larynx.

The bar alleviated these problems, the bar would be inserted into the vocal folds once they were cured and then would be placed into its holes in the stretching-pressing parts (Figure 34 – c). Details of the inserting and gluing of the bar and the vocal folds to the stretching pressing parts can be found in Materials and Methods section and in (Figure 25). The vocal folds could then freely move along the bar and were able to be elongated and shortened isotonically.

The last part was the top part (Figure 36), the function of which was to fix all the parts of the model together using screws.

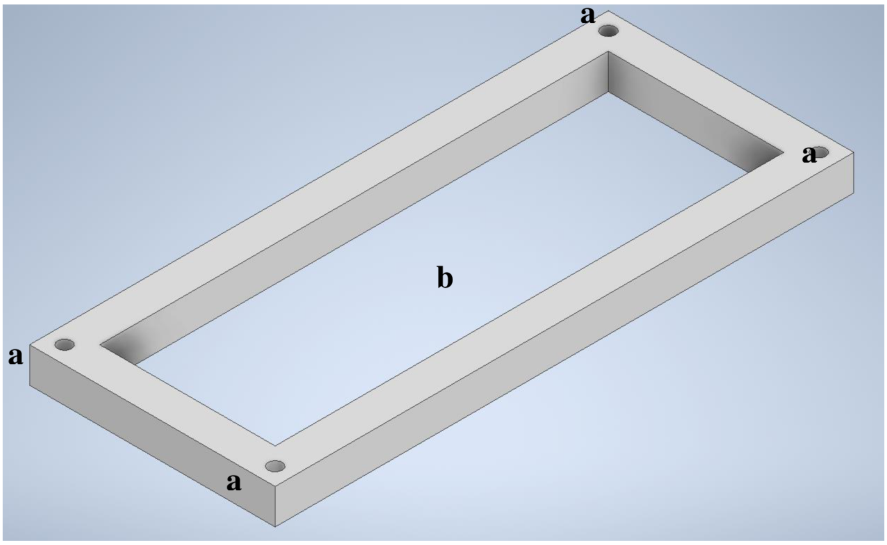

Figure 36: The top part of the supporting framework.

The top part featured four holes in its corners (a), that aligned with the holes in the bottom part and were fitted for screws meant to stabilize and fix the entire model together. Additionally, the top part was designed to allow placing an artificial vocal tract into its middle space (b) that could be used for future experiments.

5.1.2.2 Simplified version of the supporting framework

Simplified test version of the supporting framework was designed (Figure 37), to test the supporting framework and its functions while avoiding initial costly fabrication of all parts.

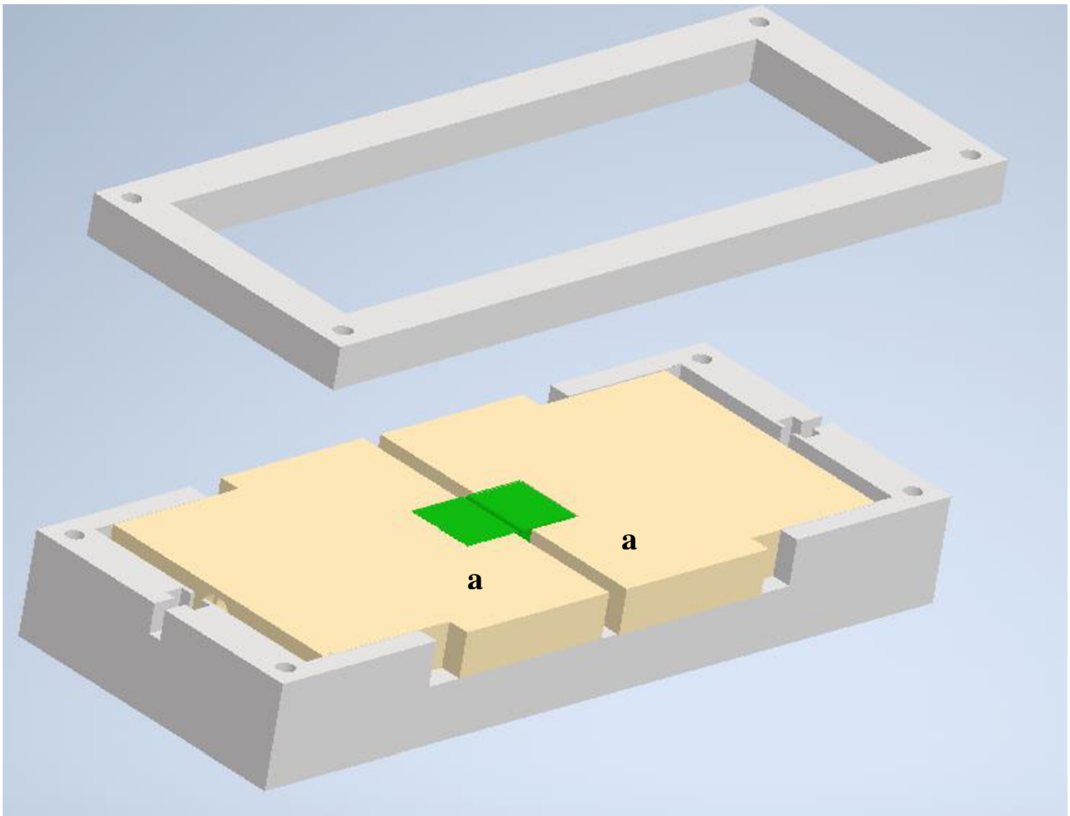

Figure 37: The virtual model of the simplified version of the supporting framework.

The simplified version of the framework had the stretching-pressing parts connected with the middle part (a), because these parts could not be 3D printed on the available 3D printer with enough precision to ensure their functionality. The vocal fold model was glued directly to the middle part (Figure 38 – a) and the bar was removed (it was not necessary here, due to inability to stretch or press the vocal folds). Additionally, precise screws could not be used for the movement of the middle part due to the same precision issues. The testing was done by placing the middle parts manually in roughly the correct position and placing the silicone cubes between them to ensure air insulation (Figure 38 - b).

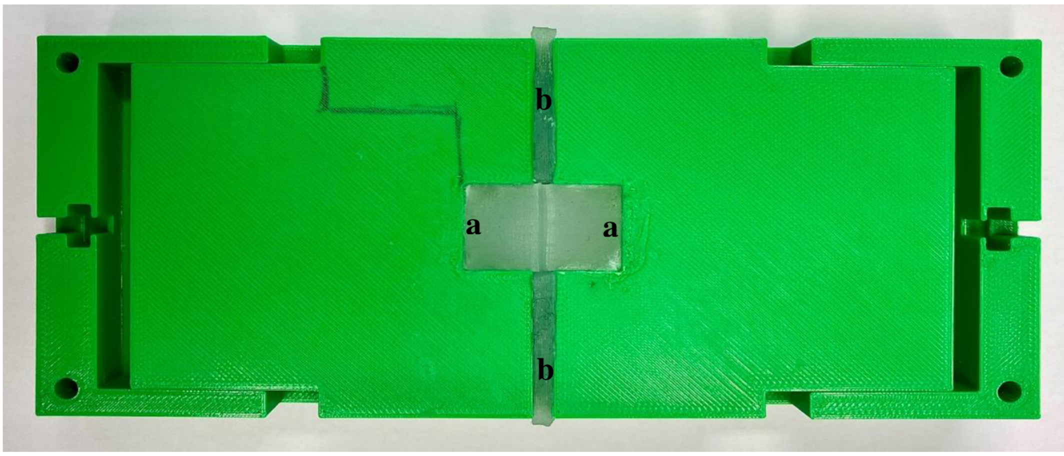

Figure 38: The simplified version of the final model used to verify the supporting framework before committing to its fabrication, featuring glued vocal fold model (a) and inserted silicone parts (b) to ensure air insulation.

5.2 Vocal fold model

5.2.1 Results of Young´s moduli measurements of silicone compounds

The first tested silicone compound was made of Ecoflex 00–30 part A, Ecoflex 00-30 part B and Silicone Thinner with ratio of 1:1:0.5 respectively. The results of the measurement can be seen in Figure 39.

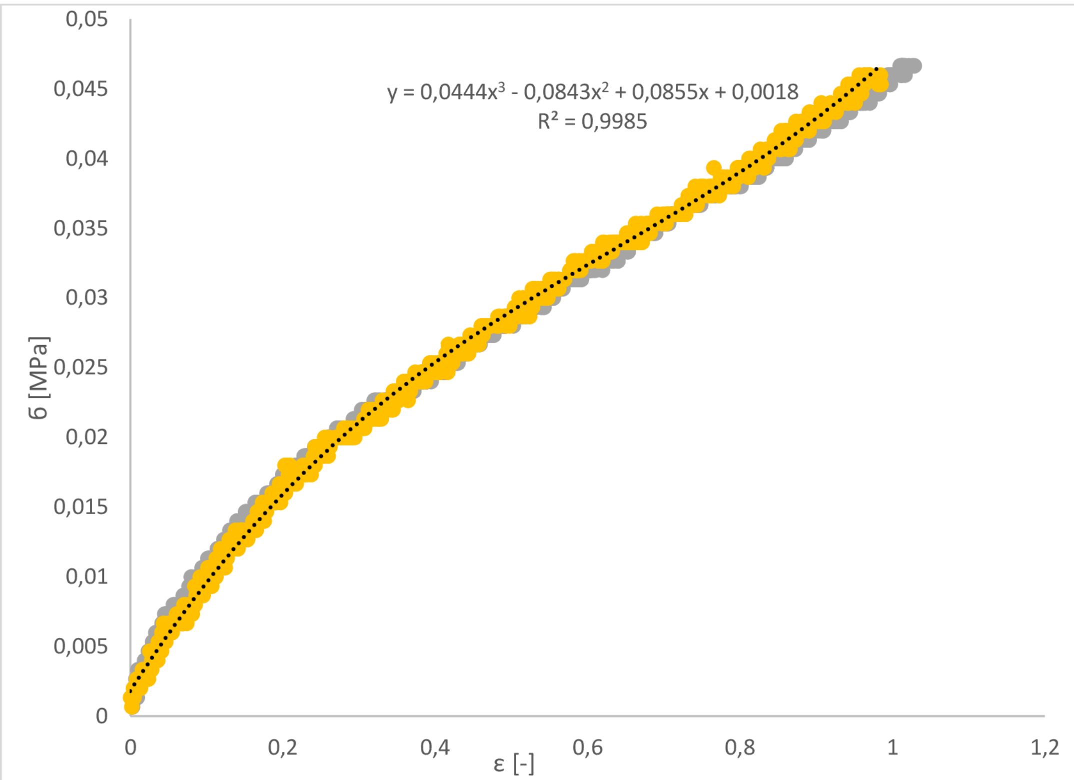

Figure 39: Stress-strain curve of the silicone compound sample with mixing ratio 1:1:0,5, fitted with a third degree polynomial function (dotted).

The Young´s modulus was calculated for elongation up to 20 %, which was decided to be sufficient for this thesis and for elongation up to 100 %, which is the value usually provided by the manufacturers. The Young´s modulus for 20% elongation was found to be 80 kPa and for 100% elongation 47 kPa. The vocal fold model made of this silicone compound showed no self-oscillation during the testing.

The second tested silicone compound was made from Ecoflex 00-30 again, this time with the ratio of 1:1:5 of Ecoflex 00-30 part A, Ecoflex 00-30 part B and Silicone Thinner respectively. The results of the measurement can be seen in Figure 40.

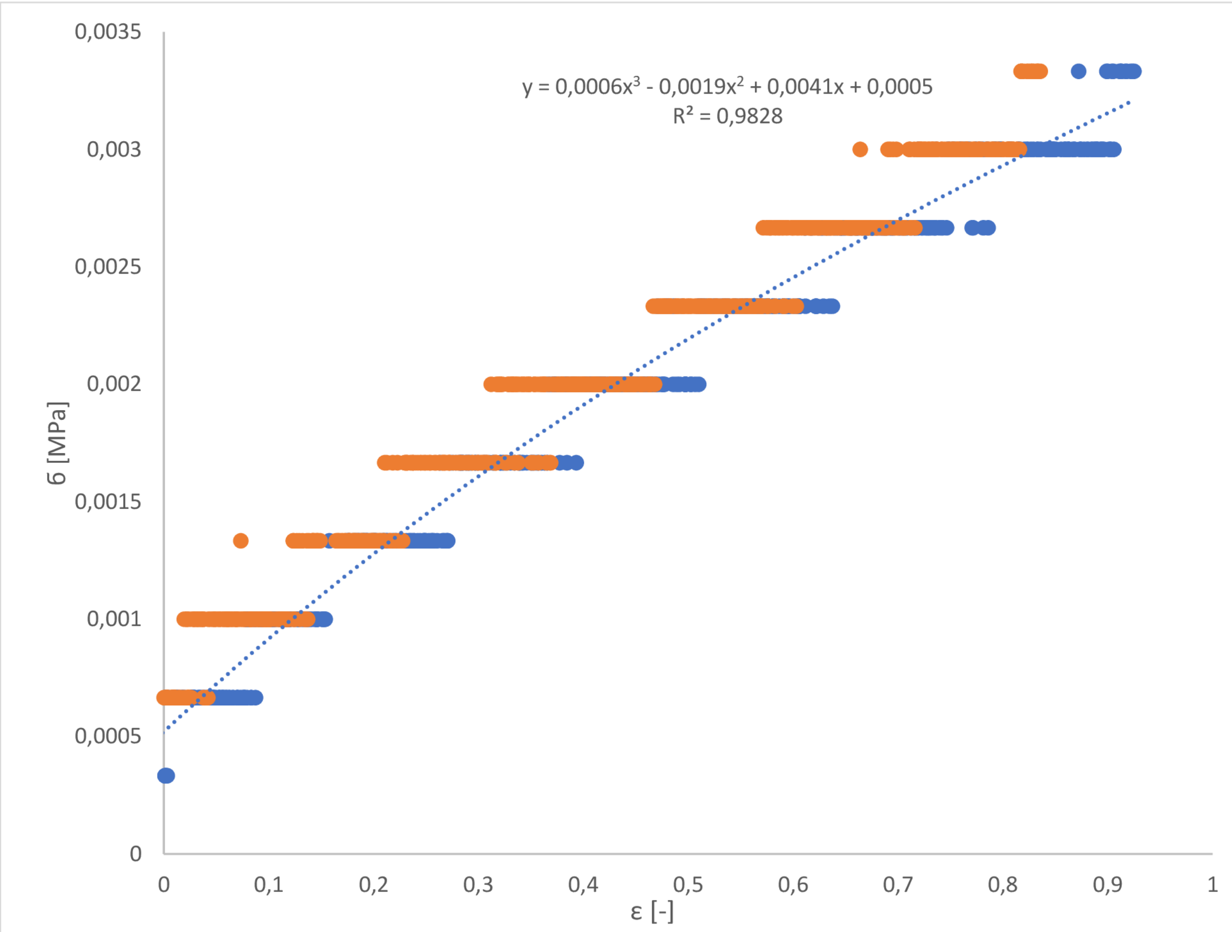

Figure 40: Stress-strain curve of the silicone compound sample with the mixing ratio 1:1:5, fitted with a third degree polynomial function (dotted).

The Young´s modulus for the second compound for 20% elongation was found to be 1,3 kPa and for 100% elongation 6 kPa. The vocal fold model made of this compound showed self-oscillation, the details are provided in the next section.

5.2.2 Tests of the vocal fold models

5.2.2.1 Vocal fold model testing on the simplified version of the supporting framework

First tests performed were made on the simplified version of the supporting framework to test the ability of the silicone vocal folds to self-oscillate.

5.2.2.1.1 Vocal fold model tests with Ecoflex 00-10

The first set of the vocal fold models tested used a silicone compound made of Ecoflex 00-10, later with addition of the Silicone Thinner to lower their Young´s modulus and viscosity. The models mixing ratios and their ability to self-oscillate are shown Table 1.

Table 1: The mixing ratios and the ability to self-oscillate of the vocal fold models made from Ecoflex 00-10. All the testing of these models was done on the simplified version of the supporting framework.

Vocal fold model number	1	2	3	4	5	6	7
Ecoflex 00-10 Part A	1	1	2	1	1	1	1
Ecoflex 00-10 Part B	1	2	1	1	1	1	1
Silicone Thinner	0	0	0	0,8	1	2	4
Self-oscillation	**none**	**none**	**none**	**none**	**none**	**none**	**none**

5.2.2.1.2 Vocal fold model tests with Ecoflex 00-30

For the next set of vocal fold models, the silicone Ecoflex 00-10 was replaced with Ecoflex 00-30, which has much lower viscosity (3000 mPa·s in Ecoflex 00-30 to 14 000 mPa·s in Ecoflex 00-10), according to the manufacturer´s product sheet. Several compounds of different mixing ratios were made, which resulted in different Young´s moduli of the compounds; the details of these compounds were described in Materials and Methods section of this thesis. Overview of the models mixing ratios, their ability to self-oscillate and the frequency of the self-oscillation are shown in Table 2, with details of the individual models following.

Table 2: The mixing ratios, the ability to self-oscillate and the frequency of self-oscillation of the vocal fold models made from Ecoflex 00-30.

Vocal fold model number	8	9	10	11	12
Version of supporting framework	simplified	simplified	simplified	simplified	final
Ecoflex 00-30 part A	1	1	1	1	1
Ecoflex 00-30 part B	1	1	1	1	1
Silicone Thinner	1	4	3	5	4
Self-oscillation	**none**	**stable**	**weak**	**stable**	**stable**
Frequency [Hz]	**none**	**90**	**iregullar**	**64**	**59**

The first Ecoflex 00-30 vocal fold model tested had a mixing ratio of 1:1:1 of Ecoflex 00-30 part A, Ecoflex 00-30 part B and Silicone Thinner respectively. This vocal fold model showed no signs of self-induced oscillation.

Next test was performed with the vocal fold model made of the same compounds, this time with the mixing ratio of 1:1:4, however. This vocal fold model showed self-induced oscillation (Figure 41). The oscillation frequency, measured using a stroboscope, was 90 Hz.

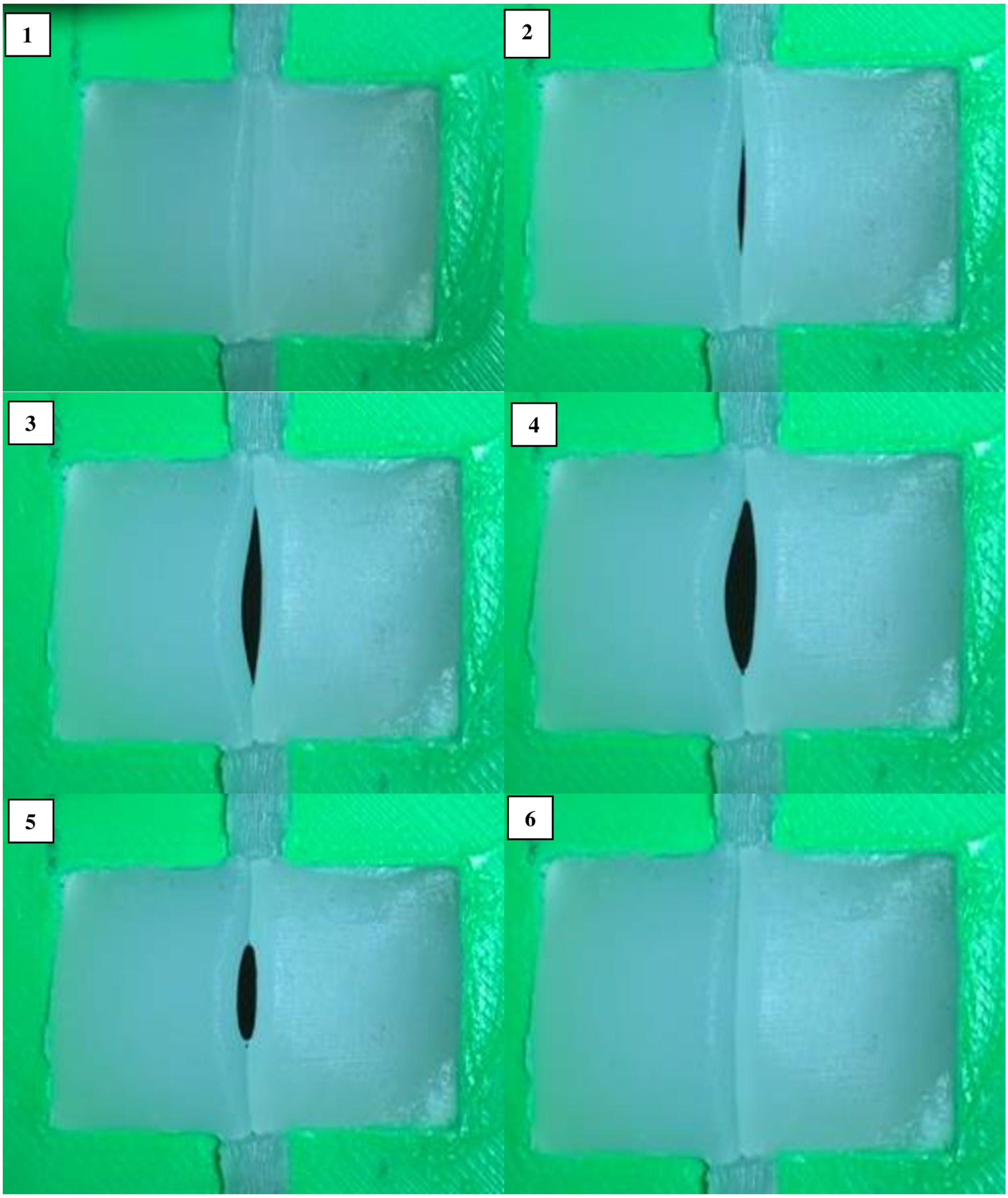

Figure 41: Screenshots from a video showing self-induced oscillation at the frequency of 90 Hz of the vocal fold model made from Ecoflex 00-30, with the mixing ratio of 1:1:4 (see the text). The vocal fold model before the oscillation began (1), during the opening phase (2 and 3), in a phase of maximum size of the glottis (4), during closing phase (5) and closed before the next opening phase began (6).

The next vocal fold model was made from the same compounds as the previous two, this time the ratio was 1:1:3. The vocal fold model showed only very weak oscillation with irregular frequency.

The last vocal fold model investigated using the simplified version of the supporting framework was mixed from the same compounds with ratio of 1:1:5. The vocal fold model showed self-induced oscillation with the stroboscope-measured frequency of 69 Hz. Measurements of the phonatory parameters were done as described in part 4.2.3. of the Materials and Methods section. The distance between the microphone and the vocal fold upper surface was 14 cm and the airflow was 1 l/s. The phonation threshold pressure for this vocal fold model was measured only approximately and was found to be ca. 8 cm H_2O. The frequency during the stable oscillation was ca. 64 Hz and the subglottal pressure during the stable phonation was 10,7 cm H_2O.

5.2.2.2 Vocal fold model testing on the final version of the supporting framework

The vocal fold model with the mixing ratio of 1:1:4 was chosen as the best model from the ones tested on the simplified version and it was decided that this model would be used for testing with the final version of the supporting framework. The vocal fold model showed self-induced oscillation (Figure 42) and measurements of the phonatory parameters were done as described in part 4.2.3 of the Material and Methods section (Figure 43).

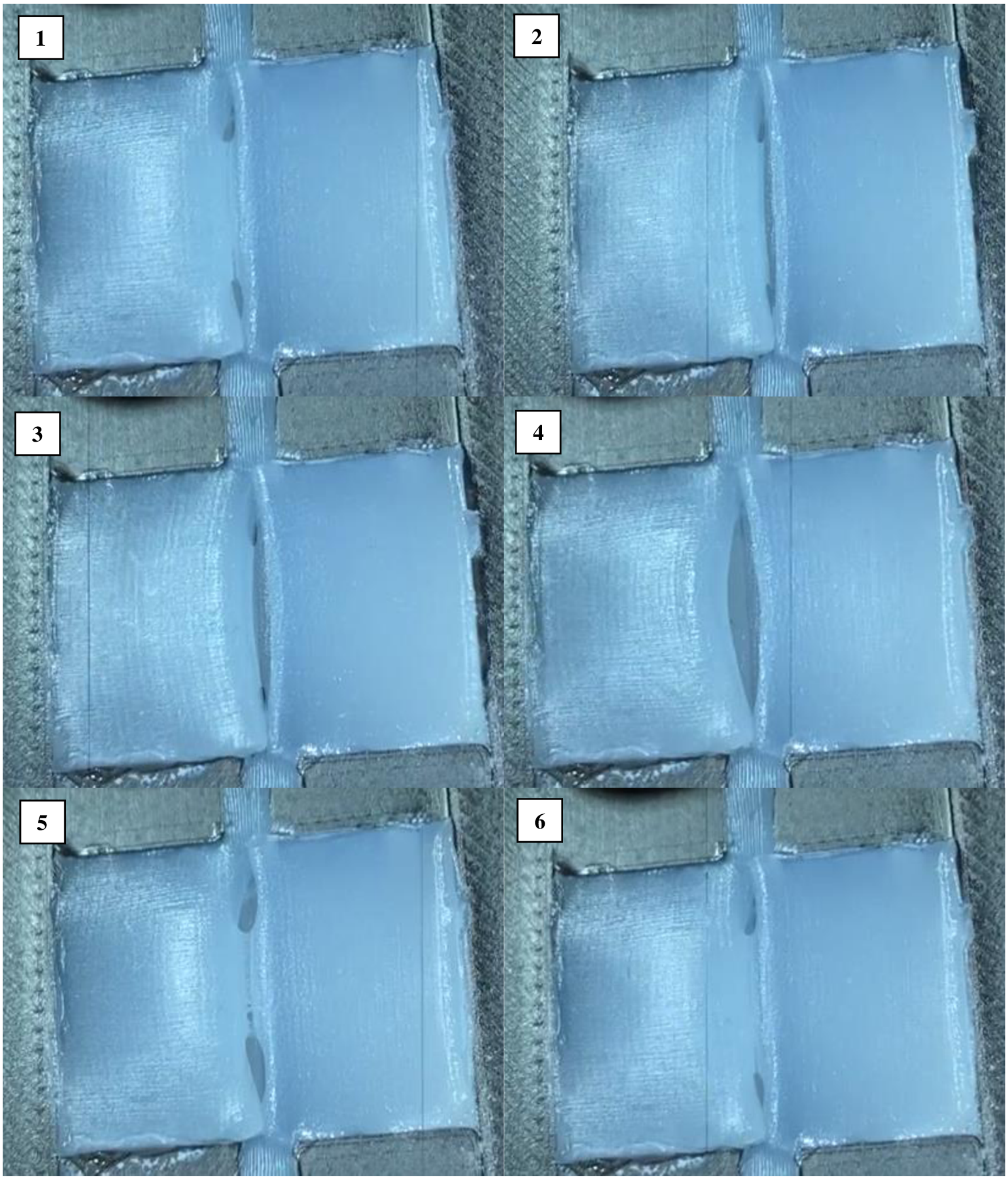

Figure 42: Screenshots from a stroboscopic video showing self-induced oscillation at the frequency of 59 Hz of the vocal fold model made from Ecoflex 00-30, with the mixing ratio of 1:1:4 (see the text). The vocal fold model before the oscillation began (1), during the opening phase (2 and 3), in a phase of maximum size of the glottis (4), during closing phase (5) and closed before the next opening phase began (6).

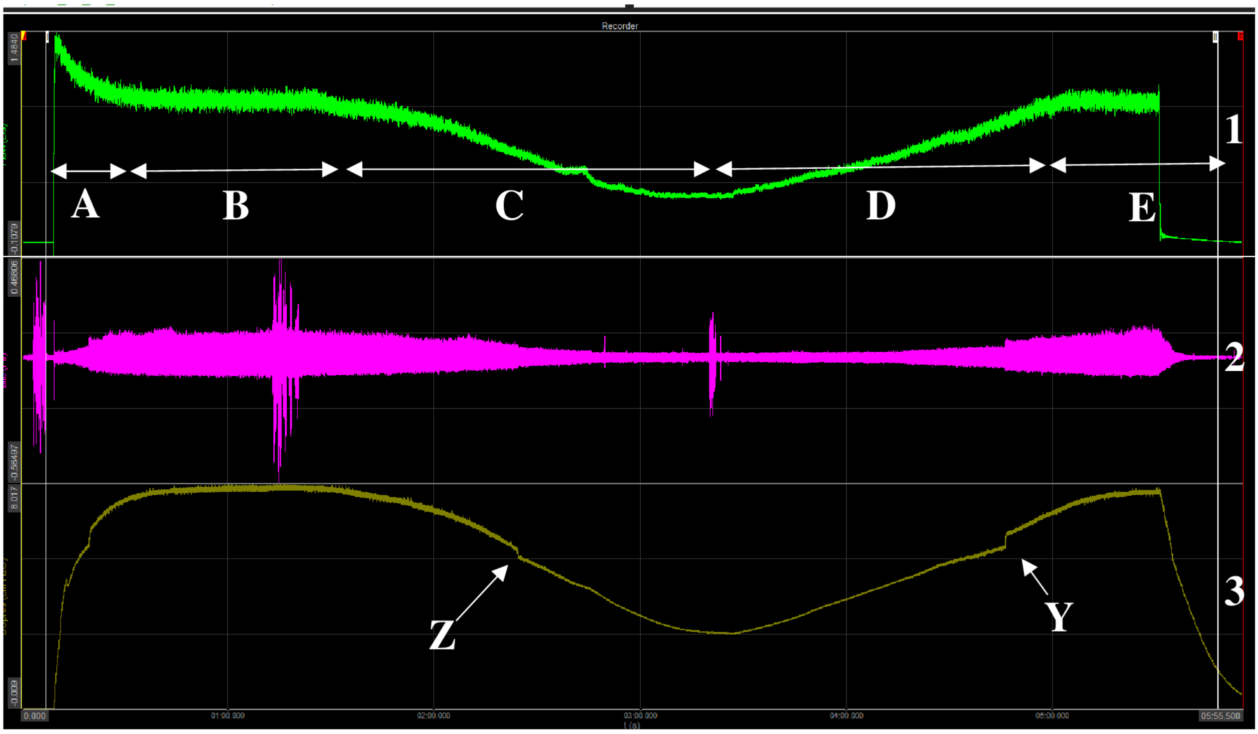

Figure 43: DewesoftX software interface showing the phonatory parameters in relation to time – airflow (1), microphone signal (2) and subglottal pressure (3). For the symbols A-E, Y and Z, see text.

Figure 43 shows the DewesoftX software interface with three graphs, displaying the airflow (1), microphone signal (2) and subglottal pressure (3) in relation to time. The first part (A) shows the airflow stabilizing after the air pump was turned on, the subglottal pressure is building up phonation and the microphone signal in this part shows only noise, which is increasing in amplitude.

In the second part (B) the airflow is stabilized at 1 l/s. In this part, stable self-oscillation of the vocal fold model was achieved at the frequency of 59 Hz, the subglottal pressure during the stable phonation was 8 cm H_2O. The peaks seen in microphone signal are the author and the supervisor talking.

During the third part (C) the airflow was slowly decreased to find the offset pressure threshold of the vocal fold model. The offset threshold pressure (Z) was found to be 5,6 cm H_2O with the corresponding airflow of 0,65 l/s. The peaks in microphone signal at the end of the third part are due to author and supervisor speaking, commenting on the state of the measurement.

In the fourth part (D), the airflow was slowly increased to find the onset pressure threshold of the vocal fold model. The onset threshold pressure (Y) was found to be 6,2 cm H_2O and the corresponding airflow was 0,86 l/s.

The first half of the last part (E) shows the once again stable phonation of the vocal fold model. In the second half, the airflow was turned off, which was accompanied by the drop in subglottal pressure and the termination of the vocal fold model´ self-oscillation.

6. DISSCUSION

The first aim of this thesis was to develop and manufacture a modular supporting framework for the silicone vocal fold model featuring important functions of human vocal folds.

The supporting framework featured the ability to open and close the glottis, simulating the abduction and adduction of real vocal folds, which is one of the most important factors during phonation. Another feature of the supporting framework was the ability to elongate or shorten the silicone vocal folds allowing to change inner tension of the vocal folds, which is another variable factor in phonation. These two features were an important part of the supporting framework. At this point, the author is not aware of any other silicone vocal fold model with its supporting framework that allows both these movements.

Another important feature of the supporting framework achieved is its modularity. The vocal fold model can be removed from the supporting framework at any time, allowing the vocal fold model to be changed for a different pair, or even just one vocal fold for another. Another modular feature of the supporting framework is the ability to remove one vocal fold and its associated supporting middle part. This feature allows replacing the half with a glass part to observe the oscillating vocal fold from the side, similarly, as done in excised hemilarynx experiments (e.g., Hiroto 1968, Jiang and Titze 1993, Berry *et al* 2001, Doellinger *et al*. 2011, Herbst *et al*. 2017). Lastly, the supporting framework was designed to allow adding artificial vocal tracts on top and to use them in further studies, similarly as done by e.g., Doellinger *et al.* (2006) or Radolf *et al.* (2016). The supporting framework was manufactured and successfully tested with silicone vocal folds. However, the initial measurements performed here didn´t use full potential of the supporting framework, therefore additional tests need to be performed to validate the supporting framework further.

The supporting framework could in future be expanded upon, e.g., by the addition of the water system developed by Horáček *et al.* and described in the theoretical part of this thesis, which would allow the usage of water filled vocal fold models, that were proven to be advantageous. Another future improvement would be the addition of the artificial vocal tract to the model the supporting framework was designed to be able to incorporate it, but this option was not tested practically.

Simplified prototype of the final version of the supporting framework was developed and manufactured to study the vocal fold models and to test the supporting framework while avoiding initial costly fabrication of all parts. The testing prototype proved to be functional, the vocal fold models could be inserted and made to self-oscillate. Another important achievement of the prototype was the insight, that a part cast from silicone, when inserted into a hole in supporting framework and made with correct dimensions, is a sufficient air insulator. These findings indicated that the final version of the supporting framework should be functional. The testing prototype could, in principle, be used in future experiments where the vocal folds wouldn´t need to be elongated or shortened. However, the testing prototype would need to be 3D printed on precise 3D printer, as the version used in this thesis showed some air leakage due to non-tight fits between the individual parts. Another limitation of the testing version is the lower modularity as opposed to the final version, because the vocal folds need to be directly glued to the supporting framework and cannot be replaced without their destruction.

The silicone compounds used for the vocal fold models were tested to measure their Young´s moduli. The silicone compound with mixing ratio of 1:1:0.5 of Ecoflex part A, Ecoflex part B and Silicone Thinner, respectively, had the Young´s modulus of 47 kPa for 20% elongation. The manufacturer provided the value of 70 kPa for the silicone without the addition of the Silicone Thinner, which seems to reflect the ability of the Silicone Thinner to considerably decrease the Young´s moduli of the compound. However, the elongation, at which the Young´s modulus was measured has not been specified by the manufacturer. The second silicone compound tested had the mixing ratio of 1:1:5 and the Young´s modulus for 20% elongation was measured to be 1,3 kPa, which shows significant decrease of the Young´s modulus with larger proportion of the Silicone Thinner. This value is similar to the Young´s moduli provided by Murray and Thomson (2011), who used the same compounds and provided the value of 1,6 kPa for the mixing ratio of 1:1:4 and the value of 0,2 kPa for the mixing ratio of 1:1:8. In the future, the silicone compound testing could proceed with measurements of viscosity and Young´s modulus of many compounds to determine the ideal range of Young´s modulus and viscosity for the single-layer vocal fold models.

Several single-layer vocal fold models made from various silicone compounds were tested on the simplified version of the supporting framework for their ability of self-oscillation. The first set of the vocal fold models tested was made from Ecoflex 00-10 silicone compound, with Ecoflex 00-10 part A and part B ratios of 1:1, 1:2 and 2:1, respectively. Neither of these showed self-oscillation. The inability to self-oscillate was attributed to their high Young´s moduli. The higher value of the Young´s modulus results in higher stiffness, which increases the phonation threshold pressure necessary for the self-oscillation to begin, as described in equation proposed by Titze *et al.* (1995) (In the original article, the equations cited is numbered as (1)). To decrease the Young´s modulus, Silicone Thinner was added to the silicone compound in several ratios; however, no vocal fold model still showed any self-oscillation. Based on the measurements performed, it was assessed, that not only is the Young´s modulus an important factor in the vocal fold model phonation, but that the viscosity of the silicone compound used for the casting also plays an important role. However, further testing is required to find the ideal viscosity for the single-layer vocal fold model.

Next step based on the conclusions of the previous experiments was to replace the Ecoflex 00-10 silicone compound with Ecoflex 00-30, which is reported by the manufacturer to have much lower viscosity. A vocal fold model was made with the addition of the Silicone Thinner in ratio of 1:1:0.5. The vocal fold model again showed no self-oscillation; therefore, higher amount of Silicone Thinner was used to decrease the Young´s modulus further.

The first model capable of self-oscillation was made with ratio of 1:1:4 of Ecoflex 00-30 part A, Ecoflex 00-30 part B and Silicone Thinner respectively. This vocal fold model showed self-oscillation at a frequency of 90 Hz, which is within the human range of phonation frequencies. Another model to show self-oscillation was made with the mixing ratio of 1:1:3. However, the self-oscillation was weak with irregular frequency, this was attributed to higher Young´s modulus compared to the previous vocal fold model. Last model tested on the simplified version of the supporting framework was made with the mixing ratio of 1:1:5 and showed self-induced oscillation at the frequency of 69 Hz. In relation to the previous assessments concerning the Young´s modulus and viscosity of the silicone compounds, the Ecoflex 00-30 with the viscosity of 3000 mPa•s, further decreased by the Silicone Thinner, fulfils both requirements of sufficient Young´s modulus and viscosity and is thus found suitable for the single-layered vocal fold models.

The last model tested was again made from Ecoflex 00-30 with the mixing ratio of 1.1:4, this time however, on the final version of the supporting framework. The model showed self-induced oscillation at frequency of 59 Hz. Measurements revealed the onset threshold pressure of 6,2 cm H_2O and the offset threshold pressure of 5,6 cm H_2O. The offset pressure threshold being lower than the onset pressure threshold corresponds with literature (e.g., Mau *et al.* 2011). The frequency of the oscillation achieved in this measurement near the lower boundary of the fundamental adult frequencies observed for lowest notes in human males (which are around 55-118 Hz as observed by Leino *et al*. 2008). It is much lower than the frequency achieved during the previous measurement done using the same silicone compound. The reason for this discrepancy is currently unknown and further testing is necessary.

In the future, more complex vocal fold models could be used, such as multi-layer vocal fold models, conductive models or models filled with liquids. The future experiments could also explore full potential of the supporting framework, such as different glottis sizes and elongation or shortening of the vocal folds.

7. CONCLUSION

This thesis was focused on development and manufacturing of a supporting framework to be used with previously developed and manufactured parts of the experimental setup and with vocal fold models in studies of phonation. Another aims of the thesis were to serve as a manual for vocal fold model fabrication and to test the manufactured single-layer vocal fold models for their ability of self-oscillation.

The supporting framework was developed and manufactured with high modularity. It was made to be compatible with the previously developed artificial trachea by means of a connector between these two parts of the experimental setup. Features of the supporting framework included the ability of abduction and adduction of the vocal fold model and the ability to change the inner tension of the vocal fold model by elongation and shortening.

Simplified testing prototype of the supporting framework was developed and manufactured to study the supporting framework´s functionality before fabricating the final complex version. The testing prototype showed functionality and the vocal fold models showed the ability to self-oscillate. Based on this, the final version of the supporting framework was manufactured and used for measurement of the phonatory parameters. The final version proved to be functional apart from some air leaks, which could be corrected by using more precise manufacturing methods.

Several vocal fold models were tested for their ability of self-oscillation. Many models showed no self-oscillation due to inappropriate materials used. Silicone compounds were later tested to measure their Young´s moduli and based on the previous tests and the measurement, a silicone compound was chosen with properties suitable for the self-oscillations to occur. The silicone vocal fold model was fabricated using the previous findings and showed self-oscillation with frequencies at the lower boundary of the human vocal fold frequency range.

The work done in this thesis was meant to provide the basis for the ability to fabricate and use silicone vocal fold models in the Voice Research Lab at the Faculty of Science of the Palacký University in Olomouc. It could be expanded upon in future; for example by the addition of artificial vocal tracts, by using more complex vocal fold models (e.g., multi-layer models, models filled with liquids, conductive models, or by exploring all of the functions of the supporting framework (e.g., different glottis size, vocal fold elongation and shortening, observation of the vocal fold motion from the side, etc.).

8. REFERENCES

Andrade P.A. (2015) *Investigations on semi-occluded vocal tract exercises in therapy and on head posture in singing*. Doctoral Dissertation, Palacký University in Olomouc, Czech Republic.

Arens C., Glanz H., Wonckhaus J-. Hersemeyer K., Kraft M. (2007) Histologic assessment of epithelial thickness in early laryngeal cancer or precursor lesions and its impact on endoscopic imaging. *Eur Arch Otorhinolaryngol* **264(6)**, 645-649.

Becker S., Kniesburges S., Muller S., Delgado A., Link G., Kaltenbacher M., Dollinger M. (2009) Flow-structure-acoustic interactions in human voice model. *The Journal of the Acoustical Society of America* **125(3)**, 1351-1361.

Berry D.A., Montequin D.W., Tayama N. (2001) High-speed digital imaging of the medial surface of the vocal folds. *Journal of the Acoustical Society of America* **110(5)**, 2539-2547.

Birkhlotz P., Gabriel F., Kurbis S., Echternach M. (2019) How the peak glottal are affects linear predictive coding-based formant estimates of vowels. *The Journal of the Acoustical Society of America* **146(1),** 223-232.

Boersma P., Weenink D. (2013) Praat: Doing phonetics by computer. Amsterdam, The Netherlands, http://www.fon.hum.uva.nl/praat/, Insitute of Phonetic Sciencies, University of Amsterdam.

Cante A., Maselli M., Nacci A., Manti M., Galli J., Paludetti G., Ursino F., Laschi C., Cianchetti M.. (2021) Conductive Silicone Vocal Folds Reproducting Electroglottographic Signal in Pathophysiological Conditions. *IEEE Transactions on Medical Robotics and Bionics* **3(2)**, 337-348.

Colton D., Monk P. (1988) The inverse scattering problem for time-harmonic acoustic waves in an inhomogeneous medium. *The quarterly Journal of Mechanics and Applied Mathematics* **41**, 97-125.

Cveticanin L. (2012) Review on Mathematical and Mechanical models of Vocal Cord. *Journal of Applied Mathematics*, **2012**, 18 pages.

De Boer B., Fitch W.T. (2010) Computer Models of Vocal Tract Evolution: An Overview and Critique. *International Society for Adaptive Behaviour* **18**, 36-47.

Deguchi S., Miyake Y., Tamura Y., Washio S. (2006) Wavelike Motion of a Mechanical Vocal Fold Model at the Onset of Self-Excited Oscillation. *Journal of Biomechanical Science and Engineering* **1**, 246-255.

Doellinger M., Berry D.A., Moentequin D.W. (2006) The influence of epilarynx area on vocal fold dynamics. *Otolaryngoloy – Head and Neck Surgery* **135(5)**, 724-729.

Doellinger M., Kobler J., Berry D.A., Mehta D.D., Leugmair G., Bohr C. (2011) Experiments on analysing voice production: Excised (human, animal) and in vivo (animal) approaches. *Current Bioinformatics* **6(3)**, 286-304.

Drechsel J.S., Thomson S.L. (2008) Influence of supragottal structures on the glottal jet exiting a two-layer synthetic, self-oscillating vocal folds model. *The Journal of the Acoustical Society of America* **123**, 4434-4445.

Fitch J.L., Holbrook A. (1970) Modal vocal fundamental frequncy of young adults. *Archives of Otolaryngology* **92(4)**, 379-382.

Gray S.D., Pignatari S.S., Harding P. (1997) Morphologic ultrastructure of anchoring fibres in normal vocal fold basement membrane zone. *Journal of Voice* **8(1)**, 48-52.

Hampala V., Švec J., Schovánek P., Mandát D. (2013). Užitný vzor č. 25585: Model subglotického traktu. (CZ 25505 U1).

Herbst C.T., Hampala V., Garcia M., Hover R., Švec J.G. (2017) Hemi-laryngeal setup for studying vocal fold vibration in three dimensions. *Journal of Visualized Experiments* **129**, 1-9.

Hiroto I. (1968) Vibration of vocal cords: an ultra high-speed cinematographic study. (Film). Kurume, Japan: Department of Otolaryngology, Kurume University)

Hirano M. (1974) Morphological Structure of the Vocal Cord as a Vibrator and its Variations. *Folia phoniatrics* **26**, 89-94.

Hirano M. (1981) Structure of vocal fold in normal and disease states: anatomical and physical studies. *ASHA reports* **11**, 11-30.

Horáček J., Šidlof P., Uruba V., Veselý J., Radolf V., Bula V., Knob M. (2008) PIV Measurement of Flow-patterng in a Human Vocal Tract Model. *Interactions and Feedbacks 2008*, NAG/DAGA 2009, Rotterdam, Netherlands, 1737-1740. Academy of Sciences of the Czech Republic, Institute of Thermomechanics,

Horáček J., Radolf V., Bula V., Košina J. (2017) Experimental Modelling of Phonation Using Artificial Models of Human Vocal Folds and Vocal Tracts. *Engineering mechanics 2017*, 23rd International Conference, May 15-18, Svratka, Czech Republic, 382-385. Brno University of Technology, Institute of Solid Mechanics, Mechatronics and Biomechanics.

Horáček J., Radolf V., Laukannen A.M. (2019) Experimental and Computational Modeling of the Effects of Voice Therapy Using Tubes. *Journal of Speech, Language, and Hearing research* **62**, 2227-2244.

Hyakutake T, Deguchi S., Shiota A., Nishoka Y., Yanase S., Washio S. (2006) Effect of Constriction Oscillation on Flow for Potential Application to Vocal Fold Mechanics: Numerical Analysis and Experiment. *Journal of Biomechanical Science and Engineering* **1(2)**, 290-303.

Ishizaka K., Flanagan J.L. (1972) Synthesis of Voiced Sounds From a Two-Mass Model of the Vocal Cords. *Bell System Technical Journal* **51(6)**, 1233-1268.

Jiang J.J., Titze I.R. (1993) A methodological study of hemilaryngeal phonation. *Laryngoscope* **103(8)**, 872-882.

Kakita Y., Hirano M., Ohmaru K. (1981) Physical properties of the vocal fold tissue: measurements on excised larynges. *Vocal Fold Physiology* **377**.

Kataoka H., Kitajima K., Owaki S. (2001) Effect of transglottal pressure on fundamental frequency of phonation: study with a rubber model. *Annals of Otology, Rhinology and Laryngology* **110**, 56-62.

Kneisburges S., Thomson S.L., Barney A., Triep M., Šidlof P., Horáček J., Brucker Ch., Becker S. (2011) *In Vitro* Experimental Investigation of Voice Production. *Current Bioinformatics* **6**, 305-322.

Kniesburges S., Thomson S.L., Barney A., Triep M., Šidlof P., Horáček J., Brúcker Ch., Becker S. (2011) In vitro experimental investigation of voice production. *Current Bioinformatics* **6**, 305-322(18).

Kucinschi B.R., Scherer R.C., De Witt K.J. Ng T.T.M. (2006) An Experimental analysis of the pressures and flow within a driven mechanical model of phonation. *Journal of the Acoustical Society of America* **119(5)**, 3011-3021.

Lehoux H., Hampala V., Švec J.G. (2021) Subglottal pressure oscillations in anechoic and resonant conditions and their influence on excised larynx phonations. *Scientifi Reports*, **11(28)**.

Leino T., Laukkanen A.M., Ilomaki I., Maki E. (2008) Assessment of vocal capacity of Finnish university students. *Folia Phoniatrica et Logopaedica* **60(4)**, 199-209.

Levendoski E.E., Leydon C., Thibeault S.L. (2014) Vocal fold epithelial barrier in health and injury: a research review. *Journal of Speech, Language, and Hearing Research* **57(5),** 1679-1691.

Miri A.K. (2014) Mechanical Characterization of Vocal Fold tissue: A Review Study. *Journal of Voice* **28**, 657-667.

Mongeau L., Franchek N., Coker C.H., Kubli R.A. (1997) Characteristic of a pulsating jet through a small modulated orifice, with application to voice production. *The Journal of the Acoustical Society of America* **102(2-1)**, 1121-1133.

Murray P.R., Thomson S.L. (2011) Synthetic, Multi-Layer, Self-Oscillating Vocal Fold Model Fabrication. *Journal of Visualized Experiments* **58**, e3498, 1-6.

Murray P.R., Thomson S.L. (2012) Vibratory responses of syntheti, self-oscillating vocal folds models. *Journal of the Acoustical Society of America* **132**, 3428-3438.

Pickup B.A., Thomson S.L. (2009) Influence of Asymmetric Stiffnes on the Structural and Aerdynamic Response of Synthetic Vocal Fold Models. *Journal of Biomechanics* **42(14)**, 2219-2225.

Pulakka H. (2005) *Analysis of Human Voice Production Using Inverse Filtering, High-Speed Imaging, and Electroglottography.* Master's Thesis, Helsinki University of Technology, Finland.

Radolf V., Horáček J., Dlask P., Otčenášek Z., Geneid A., Laukkanen A.-M. (2015) Measurement and mathematical simulation of acoustic characteristic of an arifically lenghened vocal tract. *Journal of Sound and Vibration*, **366**.Mau T., Muhlestein J., Callahan S., Weinheimer K.T., Chan R.W. (2011) Phonation threshold pressure and flow in excised human larynges. *Laryngoscope* **121(8)**, 1743-1751.

Riede T., Tokuda I. T., Munger J. B., Thomson S.L. (2008) Mammalian laryngseal air sacs add variablity to the vocal tract impedance: Physical and computational modeling. *The Journal of the Acoustical Society of America* **124**, 634-647.

Ruty N., Cisonni J., Pelorson X., Van Hirtium A., Lopez I., Hirschberg A. (2005) Experimental validation of some additional issues in physical vocal folds models. *Forum Acusticum* 741-745.

Scherer R.C., Shinwari D., De Witt K.J., Zhang Ch., Kucinshi B.R., Afjeh A.A. (2000) Intraglottal pressure profiles for symmetric and oblique glottis with a divergence angle of 10 degrees. *The Journal of the Acoustical Society of America* **109**, 1616-1630.

Scherer R.C., De Witt K.J., Kucinschi B.R. (2001) The effect of exit radii on intraglottal pressure distributions in the convergent glottis. *The Journal of the Acoustical Society of America* **110** 2267-2269.

Šidlof P. (2007) *Fluid-structure interaction in human vocal folds*. PhD thesis, Charles University in Prague, Czech Republic.

Šidlof P, Doaré O., Cadot O., Chaigne A. (2011) Measurements of flow separation in human vocal folds model. *Experiments in Fluids* **51**, 123-136.

Švec J.G., Schutte H.K., Chen C.J., Titze I.R. (2021) Integrative Insight into the Myoelastic-Aerodynamic Theory and Acoustics of Phonation. Scientific Tribute to Donald G. Miller. *Journal of voice,* Online ahead of print.

Syndergaard K.L., Dushku S., Thomson S.L. (2017) Electrically conductive synthetic vocal fold replicas for voice production research. *The Journal of the Acoustical Society of America* **142**, EL63-EL68.

TeachMeAnatomy: https://teachmeanatomy.info/neck/viscera/larynx/laryngealcartilages/ (9.2.2023)

Thomson S.L. (2004) *Fluid-structure interactions within the human larynx*. Doctoral Dissertation, Purdue University.

Thomson S.L., Mongeau L., Frankel S.H. (2005) Aerodynamic transfer of energy to the vocal folds. *The Journal of the Acoustical Society of America* **118**, 1689-1700.

Titze I.R., Schmidt S.S., Titze M.R. (1995) Phonation threshold pressure in a physical model of the vocal fold mucosa. *Journal of the Acoustical Society of America* **95(5)**, 3080-3084.

Titze I.R., Alipour F. (2006) *The Myoelastic Aerodynamic Theory of Phonation.* 1st ed. National Center for Voice and Speech, Denver.

Tran Q.T., Berke G.S., Gerrat B.R., Kreiman J. (1993) Measurement of Youngs Modulus in the in vivo human vocal folds. *Annals of Otology, Rhinology and Laryngology* **102**, 8.

Triep M., Brucker Ch., Schroder W. (2005) High-speed PIV measurements of the flow downstream of a dynamic mechanical model of the human vocal folds. *Experiments in Fluids* **39**, 232-245.

Van der Berg J., Zantema J.T., Doomenbal P. (1957) On the Air Resistance and the Bernoulli Effect of the Human Larynx. *The Journal of the Acoustical Society of America* **29**, 626-631.

Wegel R.L. (1929) Theory of vibration of the larynx. *Journal of the Acoustical Society of America* **1**, 1-21.

Weiss S., Sutor A., Ilg J., Rupitch S.J., Lerch R. (2016) Measuremen and Analysis of the Material Properties and Oscillation Characteristic of Synthetic Vocal Folds. *Acta Acustica united with Acustica* **102**, 214-229.

Zhang Z. (2016) Mechanics of human voice production and control. *The Journal of Acoustical Society of America* **140**, 2614.